UNCLASSIFIED

AD NUMBER

AD912490

NEW LIMITATION CHANGE

TO

Approved for public release, distribution unlimited

FROM

Distribution authorized to U.S. Gov't. agencies only; Test and Evaluation; 20 AUG 1973. Other requests shall be referred to Frankford Arsenal, Attn: SMUFA-L3300, Philadelphia, PA 19137.

AUTHORITY

FA D/A ltr dtd 16 Jun 1975

THIS PAGE IS UNCLASSIFIED

THIS REPORT HAS BEEN DELIMITED
AND CLEARED FOR PUBLIC RELEASE
UNDER DOD DIRECTIVE 5200.20 AND
NO RESTRICTIONS ARE IMPOSED UPON
ITS USE AND DISCLOSURE.

DISTRIBUTION STATEMENT A

APPROVED FOR PUBLIC RELEASE;
DISTRIBUTION UNLIMITED.

AD-912490

LAND CLUTTER CHARACTERISTICS FOR COMPUTER MODELING OF FIRE CONTROL RADAR SYSTEMS

EES/GIT PROJECT A-1485

Prepared for
UNITED STATES ARMY
FRANKFORD ARSENAL
PHILADELPHIA, PA. 19137
UNDER
CONTRACT DAAA 25-73-C-0256

by
R. D. Hayes and F. B. Dyer

15 May 1973

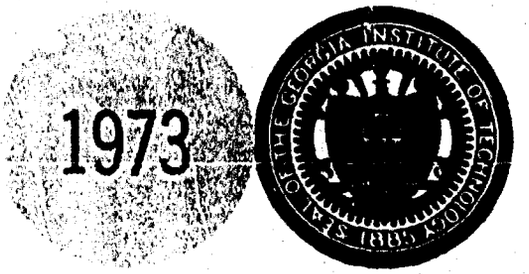

Engineering Experiment Station
GEORGIA INSTITUTE OF TECHNOLOGY
Atlanta, Georgia

GEORGIA INSTITUTE OF TECHNOLOGY
Engineering Experiment Station
Atlanta, Georgia

Technical Report Number 1
EES/GIT Project A-1485

LAND CLUTTER CHARACTERISTICS FOR COMPUTER MODELING OF FIRE CONTROL RADAR SYSTEMS

by
R. D. Hayes and F. B. Dyer

Contract Number DAAA 25-73-C-0256

15 May 1973

Distribution limited to U.S. Gov't. agencies only; Test and Evaluation; 20 AUG 1973. Other requests for this document must be referred to

Prepared for

United States Army
Frankford Arsenal
Philadelphia, Pennsylvania 19137
ATTN: SMUFA - L3300

ABSTRACT

Summarized in this report are the pertinent, unclassified data on the reflectivity of a variety of classes of land clutter. The data are confined to those taken at radar frequencies included between 9 and 95 GHz. Brief discussions are included for a number of the characteristics of radar return from clutter, although emphasis is directed to the average statistics of the amplitude of the return. Preliminary mathematical representations are included which describe: (1) average radar cross-section per unit area (σ^o), (2) amplitude statistics of the return, (3) spectral behavior of received power , and (4) polarization properties of the return from foliage. Also included is a discussion of some of the effects of the characteristics of land clutter on the choice of system parameters and on the nature of the problem of target detection in clutter.

TABLE OF CONTENTS

LIST OF FIGURES

LIST OF FIGURES (CONT.)

LIST OF TABLES

I. INTRODUCTION

A. Purpose of Study

The principal objective of the program of investigation which this report summarizes was the assembly of a basis for mathematical modeling of radar ground return at frequencies above 9 GHz. The ultimate goal of the modeling is to provide input to a computer modeling program for the description of an airborne fire control radar system. Because of the anticipated nature of the clutter return and because of the limited data base, the emphasis was placed on the assembly of a supplement to the earlier unclassified work done in radar reflectivity of ground clutter. The data assembled here have been categorized according to vegetation type, such as farmland, grass, coniferous trees, deciduous trees, and extended area returns from several basic terrain types. These data have been reduced to the same form (based on the published descriptions) insofar as possible, so that, while these data were collected by many different investigators, it is hoped that the many format problems implicit in a collection of this type have been reconciled. Considerable judgement has been used in the selection of the data reported herein; some of the selection guidelines which were used are discussed below.

B. Background

Most investigations reported have been limited to the angle region between vertical incidence and 20° from grazing. The application of radar to airborne platforms which operate at low altitudes while observing targets at long ranges requires the determination of the effects of ground clutter at angles of observation in the region from 20 degrees to zero degrees grazing. Effort has been directed to obtaining as much data and insight as possible on clutter behavior at low grazing angles.

The original sources of data used here are all more recent than the publication of the Radiation Laboratory Series and are based primarily on work done by the Naval Research Laboratory, U. S. Army Electronics Command, Ohio State University, University of New Mexico, University of Michigan, Johns Hopkins, Cornell Aeronautics Laboratory, Georgia Institute of Technology, Goodyear Aerospace, Hughes, and Westinghouse. Work reported by these groups has, in general, been supported by DOD and has remained classified for the past decade. Present policies of DOD are making this material available to the public at a very

rapid rate, and it is expected that the bulk of the data will be declassified within the next two years.

Data presented in this report have been taken from many sources, including industrial laboratories, government, and university research groups, and converted to a common nomenclature for compatable use. Great effort has been taken neither to extend nor to extrapolate any particular set of data curves, but rather to coordinate all possible data, a point at a time, and to exclude those data which do not fit with the results from other investigations. The reader is referred to the References (Section V) for the sources used. Some data are still classified and the reader is referred to the Bibliography (Section VI) for data and concepts which should be useful to extend the information presented in this report.

II. SELECTED CLUTTER CHARACTERISTICS

This section summarizes some of the clutter characteristics identified in this study. The emphasis herein is directed to description of radar cross-section per unit area, amplitude distributions of received power, and spectral properties of tree returns. Some discussions are included on the polarization properties of clutter return, primarily that from trees. Preliminary mathematical representations for σ^o and for the statistics of received power are included. Most of the discussions herein are based on observations at X-band, with extrapolations where possible using the limited data available at millimeter wave frequencies.

A. Radar Cross-Section

A large number of reports on radar reflectivity (References 1 through 21) have been reviewed and reduced to a common set of reference planes. The data are reported in a variety of differing formats and definition. Such terms as reflection coefficient, backscattering cross-section, cross-section per unit area, ground return, and terrain return are used to express the signal strength of a radar echo signal for various types of ground clutter observed with various radars under a variety of geometrical conditions.

All data presented in Figures 1, 2, 3, 4, and 5 have been reduced from the original reportings to the quantity radar cross-section per unit area, σ^o. The area observed on the ground (i.e., projected area) is limited by the radar azimuth and elevation beam widths as defined by the antenna aperture, at the higher grazing angles, and by the transmitted pulse length and azimuth beamwidth when the grazing angle, θ, approaches zero. The experimental data were checked to ensure that proper choice of projected area was used for the development of σ^o.

X-band data are considerable and are believed to be reliable. These data form the basis of discussion in the following paragraphs. From data presented by many works, it appears that the area observed, as the look-angle approaches grazing, is one of the most critical factors, perhaps more critical than absolute calibration, target description, noise levels, or exact knowledge of other system parameters. For example, data recorded with CW radars are not consistent with data recorded with pulsed systems. This is most likely due to a lack of range weighting in the "footprint" on clutter, which

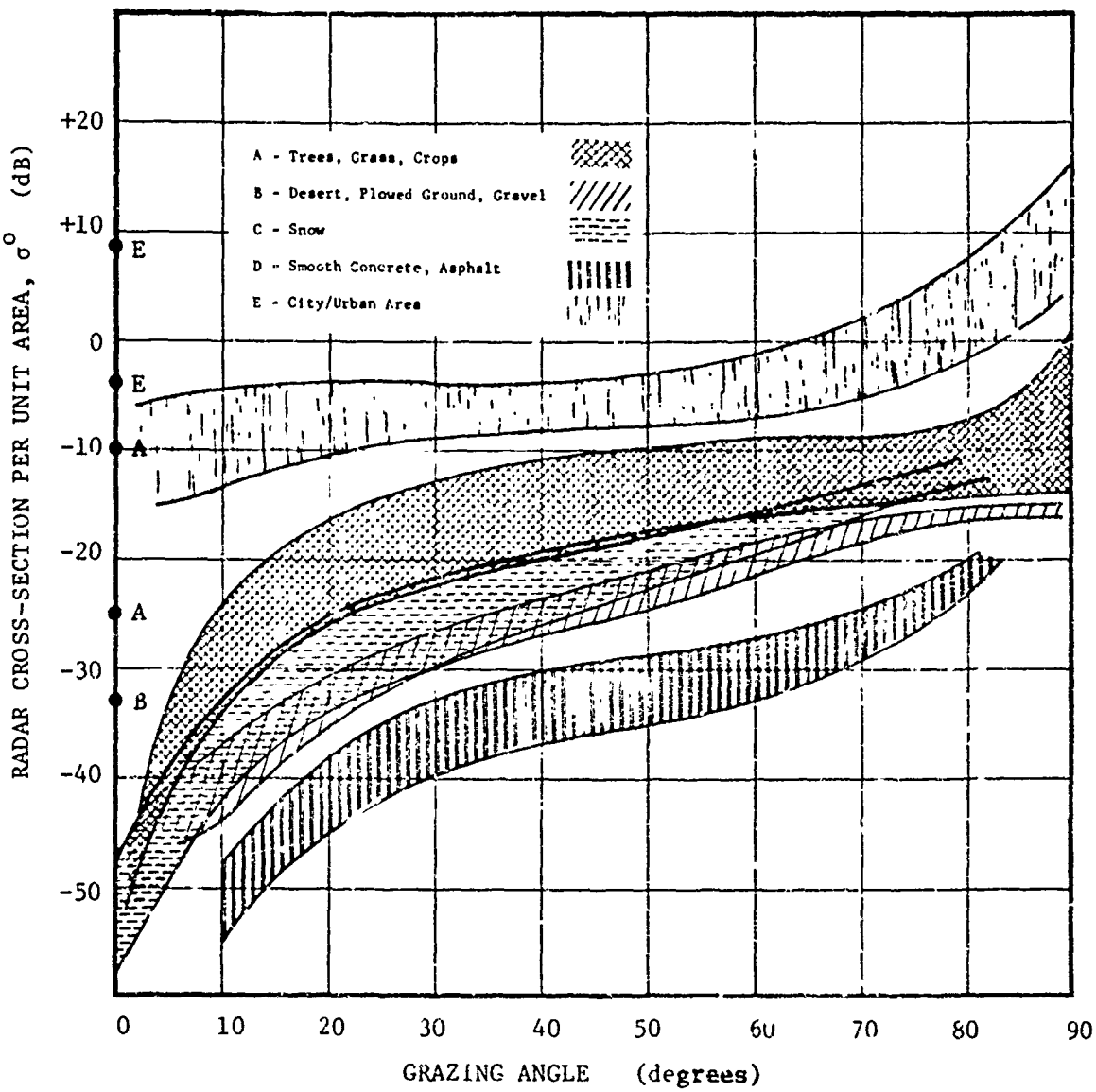

Figure 1. Radar Cross-Section of Natural Ground Targets at X-Band.

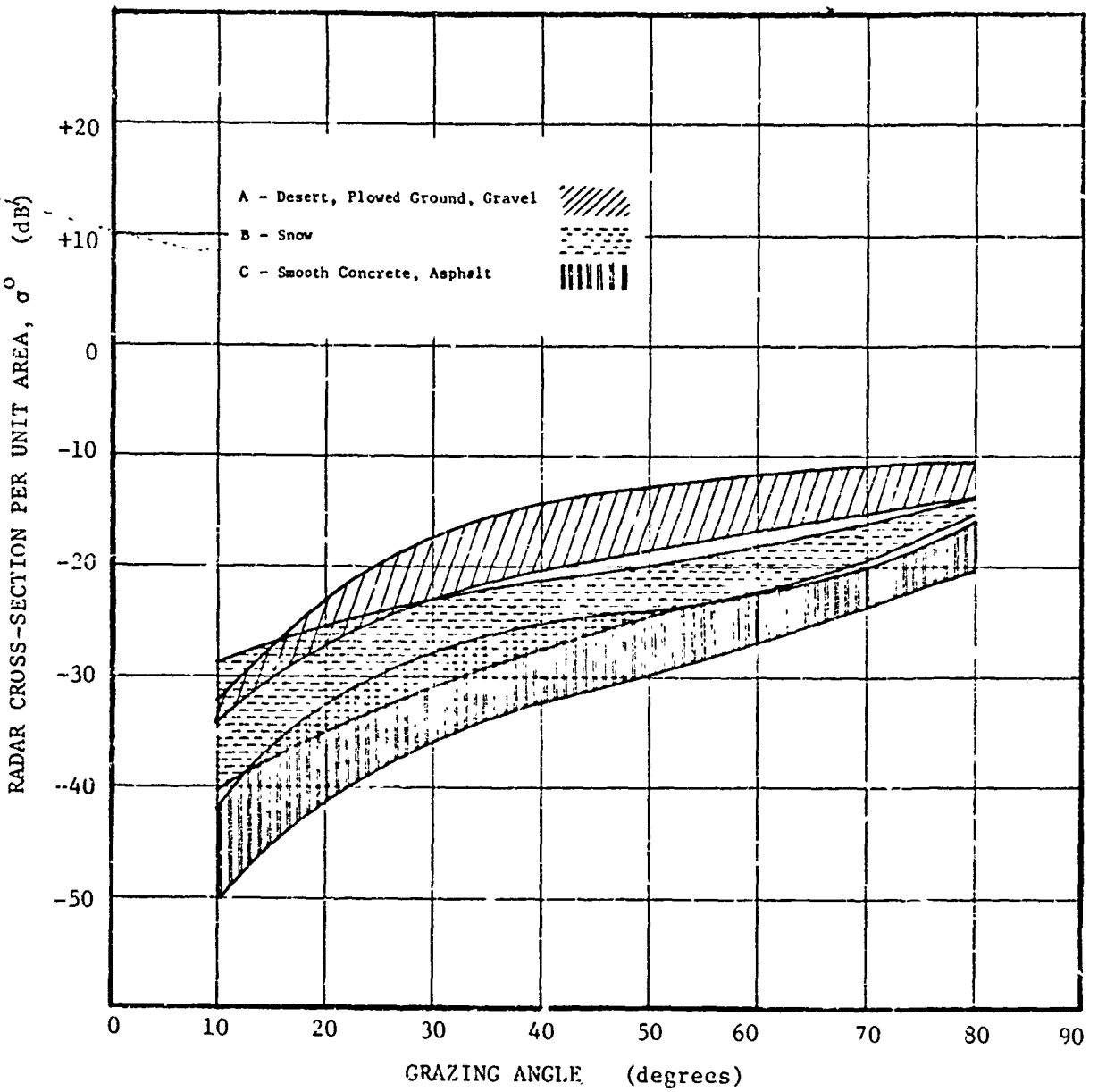

Figure 2. Radar Cross-Section of Natural Ground Targets at K_u-Band.

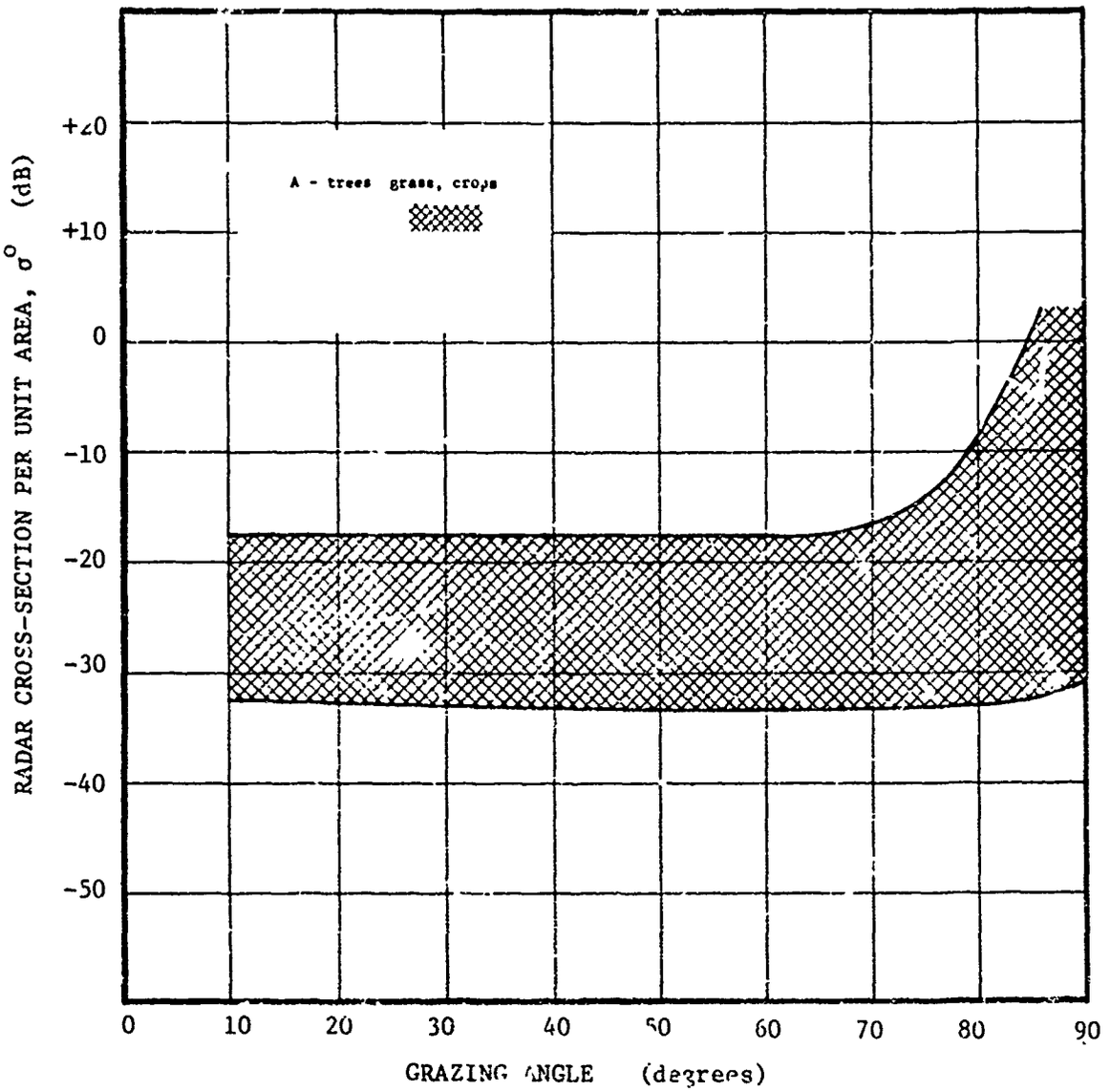

Figure 3. Radar Cross-Section of Natural Ground Targets at 24 GHz.

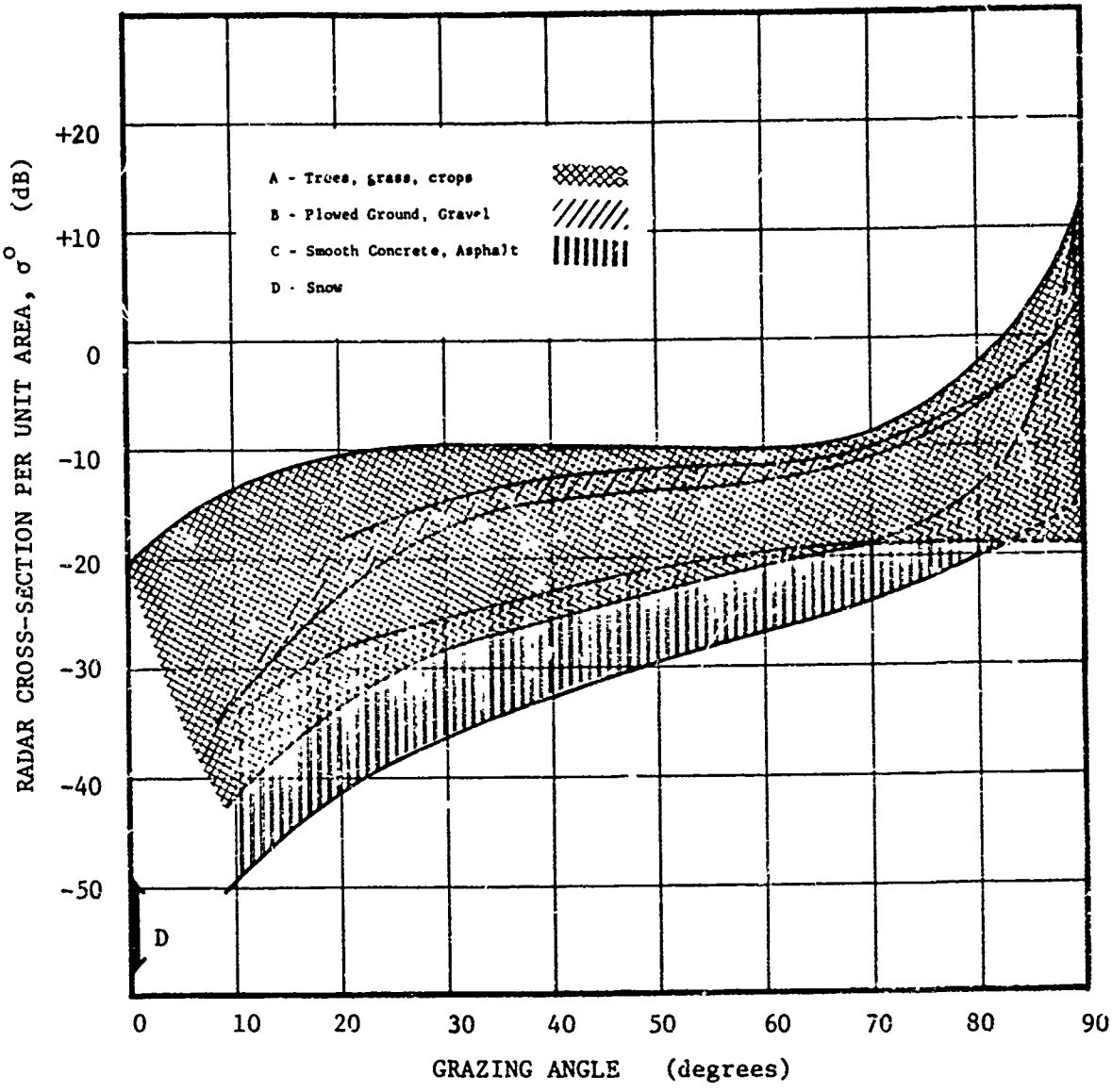

Figure 4. Radar Cross-Section of Natural Ground Targets at K_a-Band.

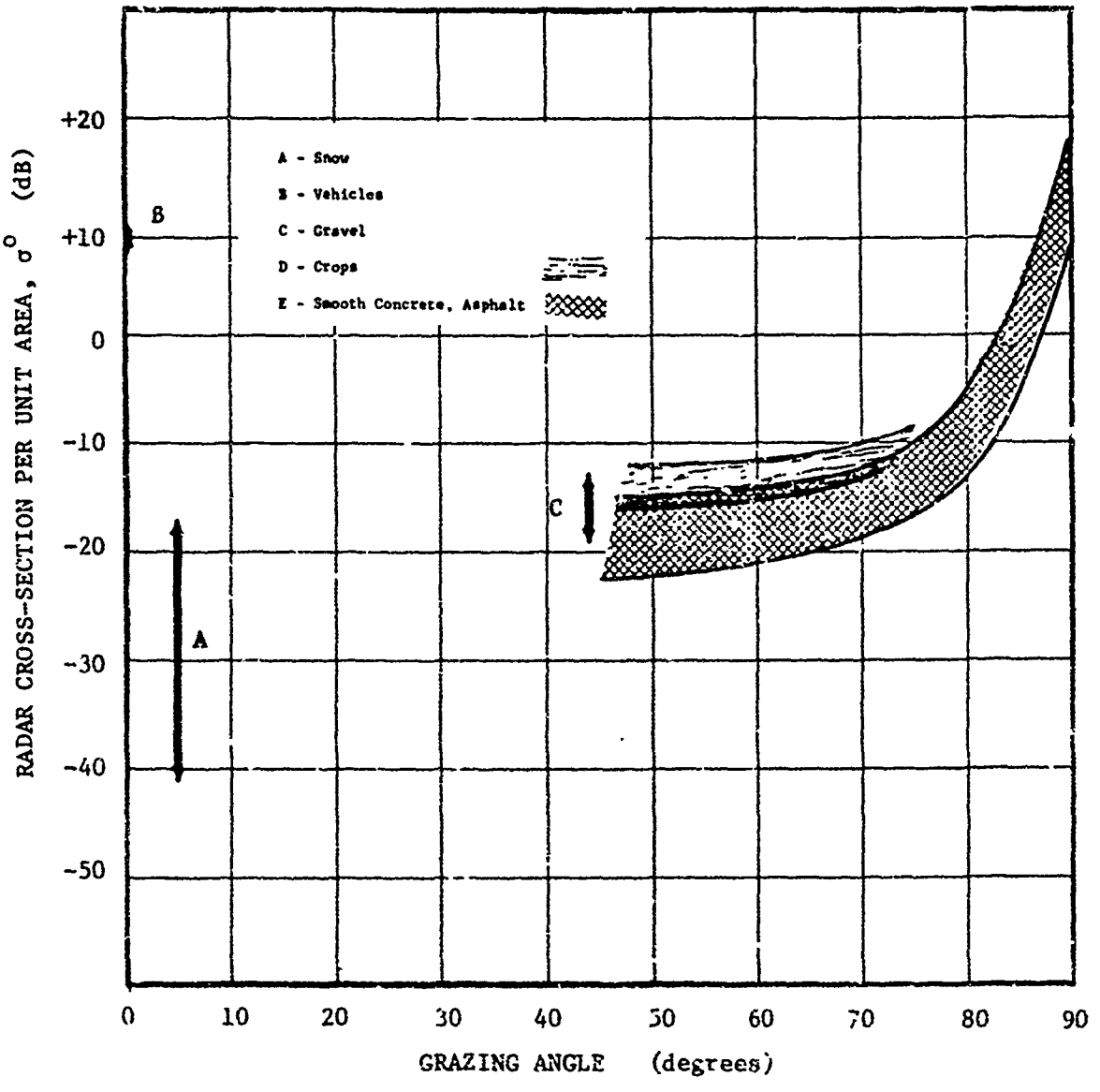

Figure 5. Radar Cross-Section of Natural Ground Targets at 40 to 90 GHz.

near grazing has a very large range variation.

From the data collected on this study, the decrease in σ^{o} as the viewing angle approaches grazing is much more rapid (20 to 25 dB) with horizontally polarized signals than with vertically polarized signal (5 to 10dB). It is not known at this time what causes this phenomenon. It could be multipath effects on uneven surfaces, changes in dielectric constant, or a lack of a true randomly polarized target area.

Surface roughness does appear to have a definable physical relationship at X-band. Some reoccurring relationships observed in the data reported by a number of experimenters are summarized in Table I.

Some natural vegetation and man-made targets were observed at angles below zero degrees. This condition occurs, for example, when the radar is located on a hillside and an exposed target area across a clearing is viewed such that the trees or buildings are actually observed at broadside. Under these conditions, the cross-section per unit area is controlled by the antenna beamwidth, not the transmitted pulse length, and the magnitude of the signal is about the same as looking straight down on the target, as expected. These values of σ^{o} are listed at zero degrees grazing angle for convenience of presentation.

As the transmitted frequency is increased, the surface variance becomes an appreciable fraction of a wavelength and the radar cross-section per unit area tends to increase. Smooth concrete tends to have the same magnitude of return as plowed ground and short crops at 35 GHz. For a given grazing angle, at 70 GHz there appear to be no natural targets with radar cross-sections as low as those observed at 10 GHz.

Insufficient data have been reported above 35 GHz to determine if the decrease in radar cross-section near grazing is as pronounced as it is at X-band.

Comparison of ground clutter at 70 degrees (approaching vertical incidence) and 20 degrees (approach grazing) has been made over the frequency range from 10 GHz to 95 GHz. Although the target areas are not the same, the general description leads one to believe that at least a first order comparison can be made. Figure 6 is a representation of average values obtained from several sources during this investigation.

It is noticed that there is a tendency for all ground clutter targets to decrease in radar cross-section after the transmitted frequency exceeds 70

TABLE I. Relationship of Surface Variance and Reported Description of Clutter

Surface Variance	Surface Description
less 1/16"	smooth concrete, asphalt fresh snow
1/16" to 1/2"	plowed ground, blown snow
1" to 4"	grass and short new crops
15" to 60'	grown crops and trees

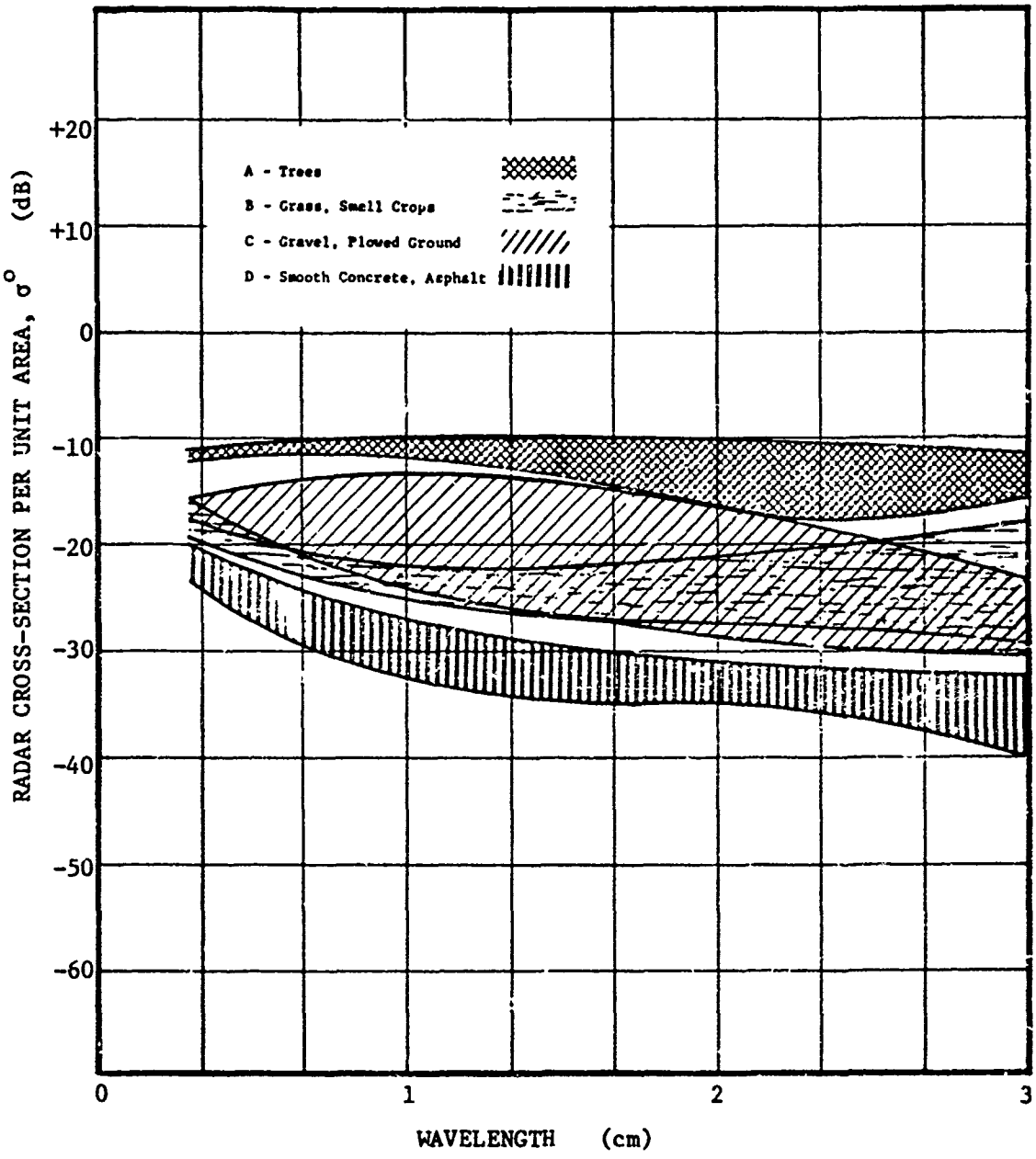

Figure 6. Clutter σ^{o} between 70^{o} and 20^{o} Grazing Angle as a Function of Wavelength.

to 80 GHz. The cause of this phenomenon is not known, however, this same tendency for the cross-section to decrease above some frequency has been observed in sea clutter. For the sea clutter case, it has been postulated that the source of reflections has changed from the wave crest/spray/droplet/facet model to some reflecting surface within the sea itself. [22]

B. Mathematical Representation of σ^o

The available data for σ^o from the various types of clutter are extremely scattered, even at X-band; however, a preliminary set of mathematical representatives for σ^o at X-band has been assembled. The expression given below is based simply on empirical data and as such should be subjected to review as new experimental data become available. In order to obtain the mathematical forms below, data from Figure 1 were replotted and further smoothed to give graphs of average values of σ^o, which were then curve-fitted. Data from Figure 6 have been used to provide a measure of the frequency scaling of σ^o for the various types of ground clutter considered here. The constants in the equations have been adjusted so that σ^o is expressed in dB, wavelength is in cm, and grazing angle is in degrees. Over the domain of wavelength considered (0.3 cm $\leq \lambda \leq$ 3 cm) and grazing angle ($0^o \leq \theta \leq 45^o$) the following form for σ^o is assumed:

$$\sigma^o = - C_1 + C_2 \log_{10} \left(\frac{\theta}{\theta_o}\right) - C_3 \log_{10} \left(\frac{\lambda}{\lambda_o}\right). \qquad (1)$$

The values of the various constants for representing each clutter type are tabulated in Table II. This mathematical representation for σ^o should be used to provide a basis for establishing average clutter background levels and as a guide to preliminary system performance assessment. More detailed data and more detailed mathematical representations are required for indepth assessment of specific processing schemes or for the exercising of extensive scenarios.

TABLE II

Tabulation of Constants Used in Mathematical Representation of Clutter (σ^o)

Clutter Type (Description)	Values of Constants				
	C_1 (dB)	C_2 (dB)	C_3 (dB)	θ_o (deg)	λ_o (cm)
Trees	11.3	26	8	35	1.0
Crops	16.3	26	8	35	1.0
Grass/small crops	20	26	10	35	1.5
Plowed ground	31	18	15	25	1.5
Gravel	28	18	15	25	1.5
Snow	25	25	15	30	1.5
Concrete	39.1	32	20	25	2.2
City/urban	6	5	3	30	1.0

C. Amplitude Distributions

Very few data have been found which describe in detail the amplitude behavior of clutter return for either a wide range of clutter types or for frequency bands above X-band. No data were found in the literature which describe simultaneous amplitude behavior at multiple frequency bands for any type of land clutter. A number of detailed descriptions of amplitude distributions were found for observations of returns from trees at X-band and these form the basis for the discussions in this section. Although a variety of formats have been presented in the literature, one of the more common formats used for displaying the data is in the form of the first probability density function, W_1, versus received power. Note the probability of finding a variable y in the range between y and $y + dy$ is given by $W_1(y)dy$, where $W_1(y)$ is called the first probability density function. Detailed W_1 information was obtained for a variety of targets and target conditions at X-band by Georgia Tech observers under an earlier program. [7] Included were observations on pine trees and deciduous trees, both wet and dry, under different seasonal foliage conditions. Typical W_1 functions have been obtained from the amplitude of the video signals and are reproduced in Figures 7 through 10.

Early investigators suggested that the amplitude distributions of various types of ground clutter could be closely approximated by a Rayleigh distribution function, that is a density function in terms of power of the form

$$P(P) = \frac{1}{< P >} e^{-P/< P >}, \qquad (2)$$

where $< P >$ represents the average power. Such a distribution occurs when the received signal is the vector sum of the echoes from a large number of independently moving small scattering elements adding in random phase, and the average amplitude of the component echoes from individual scatterers is constant. However, careful experimental determination of the first probability density functions of clutter echoes showed significant deviations from the Rayleigh form, especially in the high amplitude "tail". An example of the type of theoretical investigations that has been made in order to determine a physical mechanism to account for the observed W_1 distributions in terms of Rayleigh functions is described below.

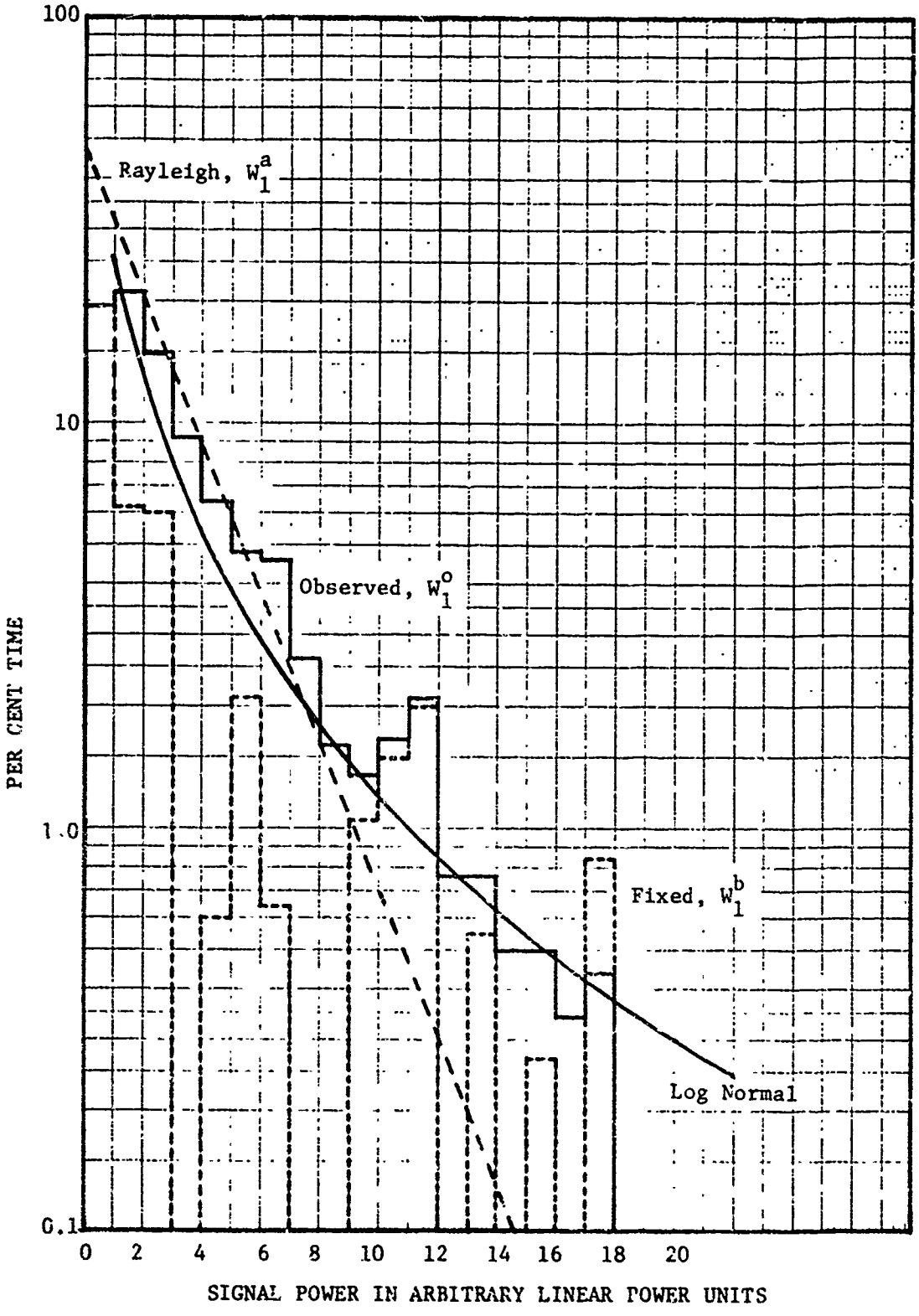

Figure 7. First Probability Distribution of Power of Deciduous Tree Return. Horizontal Transmission and Reception. (Hayes, et al., Ref. 7)

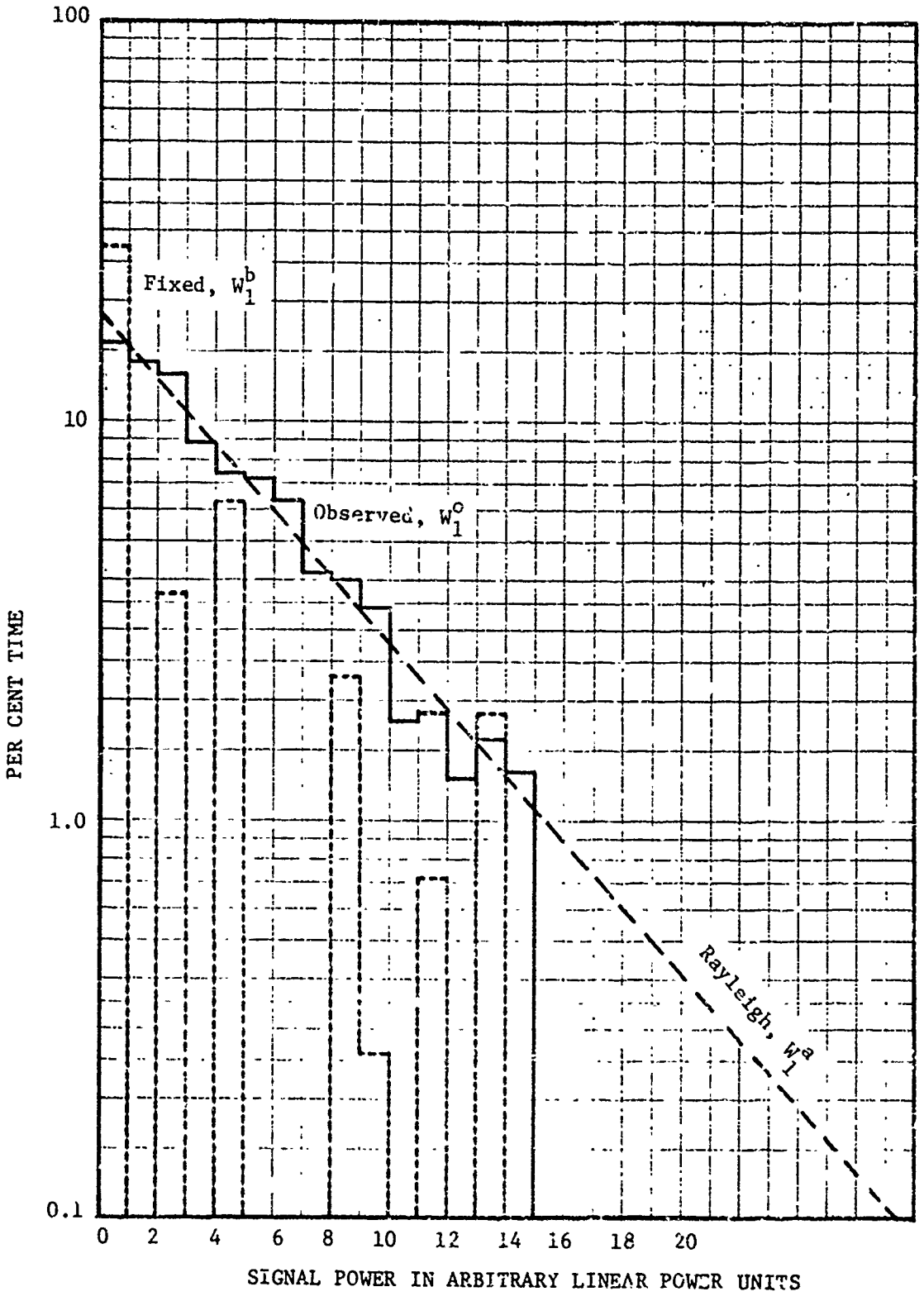

Figure 8. First Probability Distribution of Power of Deciduous Tree Return. Horizontal Transmission, Vertical Reception. (Hayes, et al., Ref. 7)

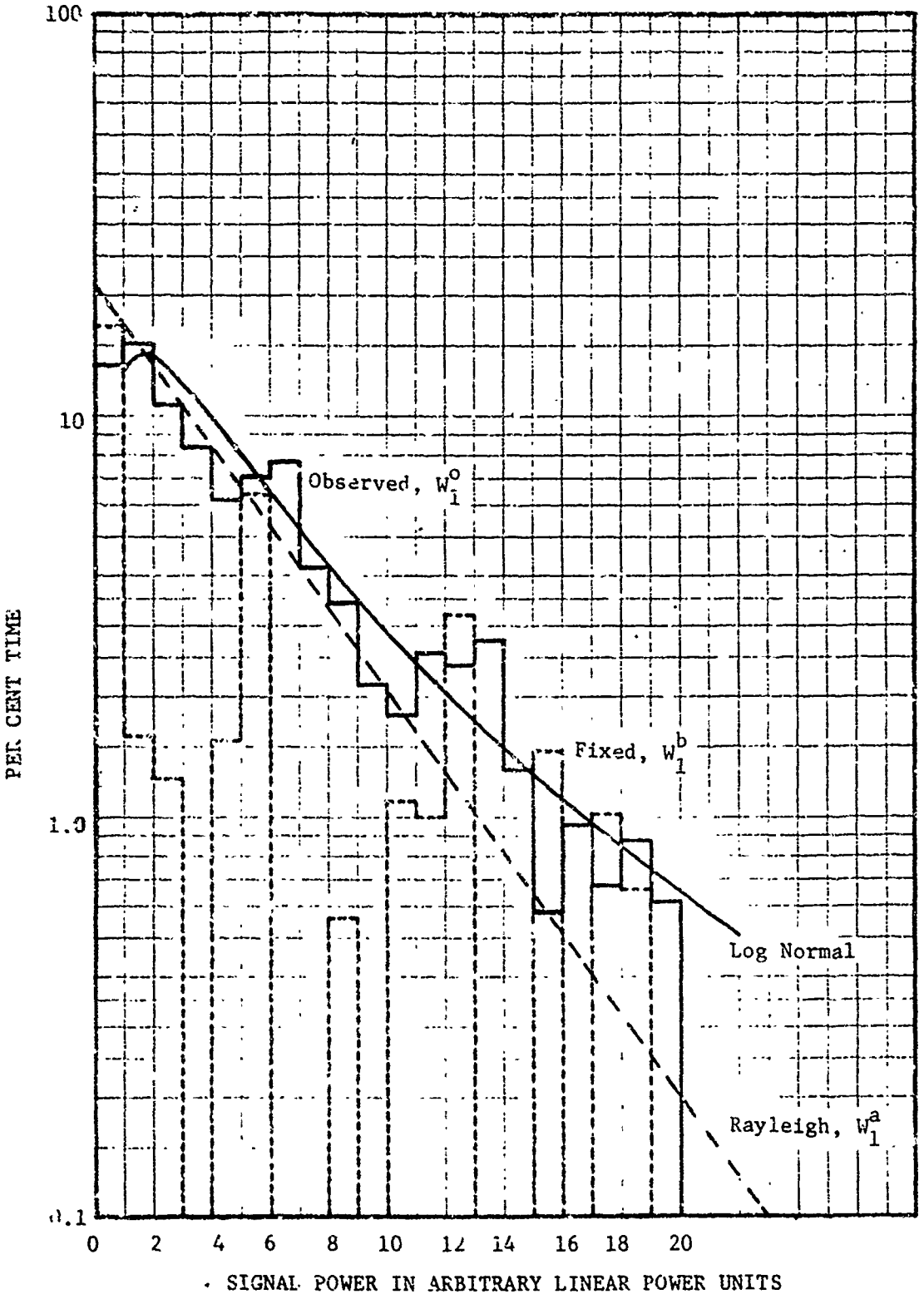

Figure 9. First Probability Distribution of Power of Pine Tree Return. Right Circular Transmission and Reception. (Hayes, et al., Ref. 7)

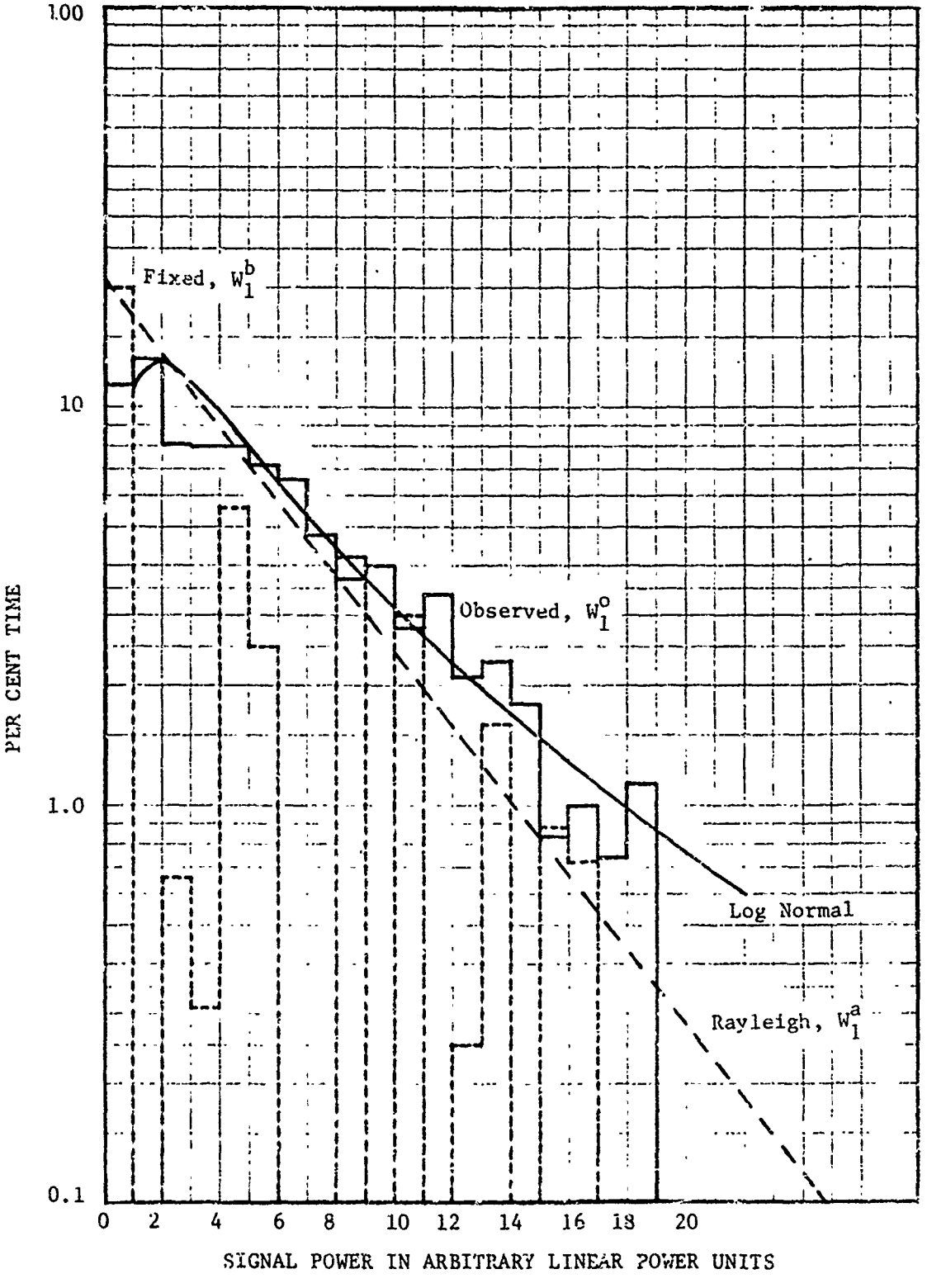

Figure 10. First Probability Distribution of Power of Pine Tree Return. Right Circular Transmission, Left Circular Reception. (Hayes, et al., Ref. 7)

Assume that two independent echo mechanisms, whose signals add, are simultaneously present. Then the observed first probability density function is given by the convolution of the probability density functions of the two mechanisms. [24] Mathematically,

$$W_1^{o}(P) = \int_0^P W_1^{a}(P - x)\, W_1^{b}(x)\, dx. \tag{3}$$

Now assume that W_1^{a} is a Rayleigh density function and W_1^{b} is unknown. Then

$$W_1^{o}(P) = \int_0^P \frac{e^{-(P - x)/< P >}}{< P >} W_1^{b}(x)\, dx. \tag{4}$$

Differentiating, [25]

$$\frac{dW_1^{o}(P)}{dP} = \int_0^P \frac{\partial}{\partial P} \frac{e^{-(P - x)/< P >}}{< P >} W_1^{b}(x)dx + \left[\frac{e^{-(P - x)/< P >}}{< P >} W_1^{b}(x) \right]_{x = P}$$

$$= -\int_0^P \frac{e^{-(P - x)/< P >}}{< P >^2} W_1^{b}(x)\, dx + \frac{1}{<P>} W_1^{b}(P)$$

$$= -\frac{1}{<P>} W_1^{o}(P) + \frac{1}{< P >} W_1^{b}(P) \tag{5}$$

Thus,

$$W_1^{b}(P) = W_1^{o}(P) + < P > \frac{dW_1^{o}(P)}{dP} \tag{6}$$

This means that the density function of the unknown mechanism can be determined from the observed density function and its derivative. This process was applied to data collected on former projects to determine if a simple physical interpretation could be assigned to the results. The difficulty in using Equation (6) lies in the determination of $< P >$. Note that $< P >$ represents the average power in the Rayleigh function, not the observed distribution. As the value of W_1^b (P, at any point depends critically on both the derivative of the observed density function at that point and the average power of Rayleigh function, it is essential to get good estimates of both these quantities. A bad estimate of either can lead to negative values for some of the calculated points on the W_1^b (P) curve, which, of course, is a nonsensical result. It is the difficulty in estimating the average power of the Rayleigh density function which limited the application of this separation process to clutter runs already closely approximating the Rayleigh form. The dashed lines in Figures 7 through 10 show the results of applying the process to the observed density functions shown as solid lines. The straight lines on the observed density functions for clutter targets consist of a Rayleigh distributed return plus the returns from several constant targets of different magnitudes which are illuminated only part of the time. From some of the other data collected which are not reproduced here, it would appear that sometimes a second Rayleigh type target is also present. It is postulated that the leaves and twigs produce the Rayleigh return, while the tree trunks and branches correspond to the constant targets which are intermittently illuminated.

Many observers are currently proposing log-normal distributions as mathematical representations for both ground and sea clutter radar return. [26] The log-normal distribution allows for larger values of peak power than the Rayleigh for a given median, and, since its standard form allows the use of well-defined mathematical expressions, its usefulness to engineers is clear.

Log-normal curves have been drawn on Figures 7, 9, and 10. A similar fit was not attempted for Figure 8, as the Rayleigh distribution appears to be adequate. It appears that with proper selection of the mean value and standard deviation, a good fit to the data can be obtained. The most obvious limitation in its fit occurs in the failure to predict the truncation of returns at high power levels. This truncation can be expected to occur under all circumstances, since all targets have some upper limit on cross-section; however, none of the simple mathematical forms actually follow this behavior.

Mathematically, the log-normal distribution can be represented by a function of the form

$$P(P_c) = \frac{1}{\sqrt{2\pi}\,\sigma\,P_c} \exp\left[-\frac{1}{2\sigma^2}\left(\ln\left(\frac{P_c}{P_m}\right)\right)^2\right], \qquad (7)$$

where P_c is the received power from the clutter, P_m is the median value of P_c, and σ is the standard deviation of $\ln P_c$. Many authors use the parameters $\overline{P}_c$, mean signal, and ρ, the ratio of mean to median, to characterize a given log-normal distribution. [26, 27] In terms of σ and $\ln P_m$ these parameters are

$$\overline{P}_c = \exp\left[\frac{\sigma^2}{2} + \ln P_m\right] \qquad (8)$$

and

$$\rho = \exp\left[\frac{\sigma^2}{2}\right]. \qquad (9)$$

The corresponding values for σ, ρ, and $\overline{P}_c$ for the log-normal curves in Figures 7, 9, and 10 are given in Table III. The rationale for the use of the log-normal distribution as a representation of radar return is discussed in several texts. The physical interpretation of the log-normal distribution is described by Aitchison and Brown [28]; however, in general the expected log-normal distribution results from a large collection of scatterers which vary from very small to large cross-sections. [27, 28]

D. Spectral Properties

1. Windspeed Effects on Tree Return

No data have been presented with exact wind speed information correlated with amplitude of radar return. The basic problem with those measurements which have been reported is that wind speed is usually measured at the radar, thus the large range separation between the radar and the trees results in a poor knowledge of the wind at the trees. However, when the measurements have been made at the trees, reflections from the mast, rotating cups and vane, making up the anemometer system influence the clutter returns. In one investigation, the wind equipment was located in a cleared area, within a few hundred feet of the measurement system and in a direction which would produce the best indication of the wind conditions at the clutter area. With this arrangement exact wind conditions were recordable for a finite time interval only if the

TABLE III

Log-Normal Parameter Values for Tree Returns

Parameter	Value		
	HH (Figure 7)	RR (Figure 9)	RL (Figure 10)
σ	6.51 dB	4.34 dB	4.34 dB
ρ	3.08	1.65	1.65
$\overline{P}_c$	4.62	7.42	8.24

wind was constant, and this was rarely encountered for windspreads above 6 mph.

Data collected from dry pine trees while transmitting horizontal polarization were examined for a relationship between windspeed and change in amplitude. In a 10-second interval, the difference between the maximum and minimum amplitudes for both parallel and cross returns ranged from 23 to 28 dB for runs with windspeeds ranging from 0 to 13 mph. For the most part, at windspeeds below 4 mph the amplitude of the signal changed with a gradual slope, but changes of 14 dB in less than 1/10 second were observed. When these occurred, the signal would not go through large changes of magnitude in rapid succession, rather, the signal would first be fairly constant, then make a sharp change in amplitude and vary in a gradual manner about this new level before further rapid changes. For a wavelength of 3 cm, windspeeds of less than 4 mph are sufficient to cause leaves to move distances of $\lambda/2$ in a spasmodic manner and thus produce the variation in amplitude noted above. Although no correlation is apparent between windspeed and the difference between maximum and minimum amplitude of return signals in a 10-second interval, a relationship might be discovered if the change in amplitude could be examined for very short intervals, something less than 1/100 second.

The data were also examined for a relationship between windspeed and the rate of fluctuation of the signal without regard to the amplitude of the fluctuation. For this analysis, a fluctuation is defined as a change in the slope of the echo amplitude from positive to negative. The number of fluctuations will, of course, be a function of the response of the observing system. The measurements radar has a flat frequency-amplitude response from 0 to 500 cps; however, the data system, for this test, has a flat response from 0 to 100 cps. Thus the data presented in Figure 11 may be considered as relative fluctuations.

From this figure, it is noted that the increase is of the same general type whether observing the parallel return or the cross return. Each bar or dotted area represents the range of fluctuations from 2-second observations and a curve has been drawn through these bars and areas to obtain an estimated average relationship. There is a sharp increase when the windspeed is near 10 mph; apparently this corresponds to the windspeed which causes small twigs and leaves to be in constant motion. Accepted standard specifications for estimating wind velocity by observing the condition of objects in the surrounding area are listed in Table IV.

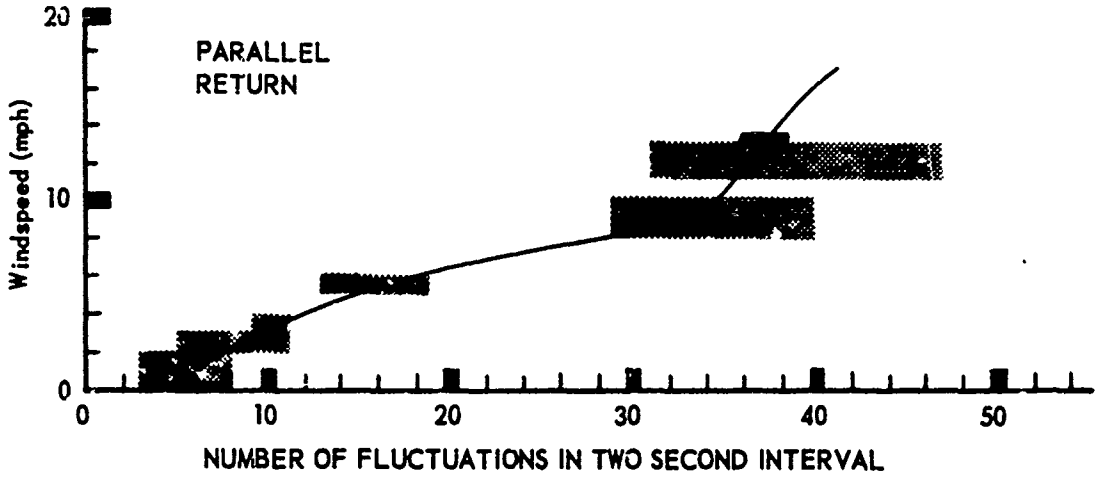

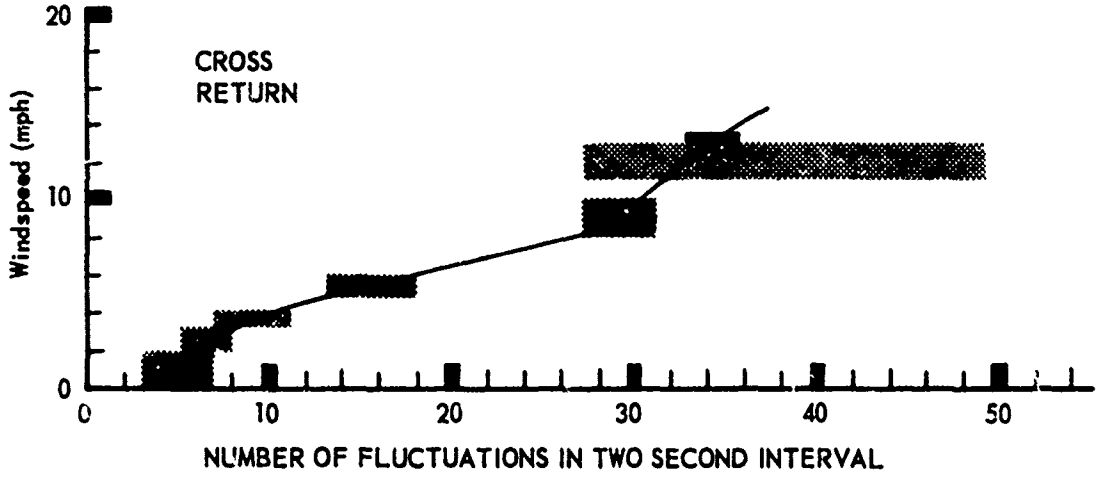

Figure 11. Relative Number of Fluctuations in Parallel and Cross Returns from Dry Pine Trees as a Function of Windspeed. Horizontal Transmission.

TABLE IV.

Standard Specifications for Estimating Wind Velocity

Velocity (mph)	Specifications for estimating velocity*
less than 1	Smoke rises vertically
1 to 3	Direction of wind shown by smoke drift but not by wind vanes
4 to 7	Wind felt on face; leaves rustle; ordinary vane moved by wind
5 to 12	Leaves and small twigs in constant motion; wind extends light flag
13 to 18	Raises dust and loose paper; small branches are moved

*Army Air Forces TM 1-235, June 1942, p. 193.

When the radar was trained on the side of a hill containing deciduous trees, the average signal level was frequently observed to change with windspeed. In general, indications are that the average return increases when the windspeed drops from a value in the vicinity of 10 mph to a value of less than 4 mph. Phenomena similar to this have been seen on other occasions where mixtures of fixed and fluctuating targets were observed.

The number of fluctuations for vertically polarized transmission has been observed to be lower than that for horizontally polarized transmission, and in general the number for circularly polarized transmissions is lower than linearly polarized transmissions. Also for a given windspeed, the number of fluctuations is less when the trees are wet than when they are dry.

In the windspeed range of 4 to 14 mph, returns from dry pine trees show the number of fluctuations in a two-second interval to increase with increase in windspeed for both the parallel and cross returns, but the ratio of parallel to cross return shows no dependence on windspeed. Also, the magnitude of the linear correlation coefficient between parallel- and cross-polarized echoes was usually below 0.3 for linearly polarized transmissions.

2. Doppler Return for Ground Clutter

A few power density spectrums from clutter returns have been recorded and analyzed at X-band; however, no detailed investigations have been reported at frequencies above 10 GHz. Almost without exception, those observations which have been made indicate that there are more high frequency components in the return signals than accounted for by the use of the Gaussian distribution. [20] For example, Fishbein [21], suggested that a cubic relation between power density and frequency is a better fit to the data than a Gaussian distribution. Other investigators have suggested that a 4th power relationship would be an even better fit to the actual recorded data. Following Fishbein:

$$W(f) = \frac{1}{1 + (\frac{f}{f_c})^3} \tag{10}$$

where

$$f_c = ke^{\beta v}$$

$$k = 1.334 \quad \beta = 0.356 \text{ (knots)}^{-1}$$

$$v = \text{windspeed (knots)}$$

In each of the suggested functions, there is an unknown which is best determined from actual recorded data. For the Gaussian, it is necessary to determine the standard deviation; for the power functions it is necessary to determine the corner frequency, f_c, or the half-power point. From the data recorded and presented in Figure 12, it does appear that the Gaussian distribution does not fit the data, due to a rapid fall off at high frequencies. The relationship suggested by Fishbein is a good fit, as is the fourth-power relationship. In applications requiring the filtering of the terrain clutter Doppler while retaining the target Doppler, improved filter designs may be obtained if the clutter is assumed to have the fourth-power relationship. This assumption may result in significantly better processor performance, especially if the improved filters are used with a optimum choice of polarization.

3. Linear Correlation Coefficients

The linear correlation coefficient is a measure of the strength of the linear relationship between two variables. The magnitude of the coefficient is an indication of the strength of this relationship and the sign of the coefficient determines the relative phase between the two variables. When the correlation coefficient is +1, the relationship between the variables is linear and the variables are in phase. When the correlation coefficient is -1, the relationship is linear and the variables are out of phase by 180 degrees. When the coefficient is zero, no linear relationship exists between the two variables. The coefficient is, of course, independent of the absolute magnitude of either variable.

In application to the radar problem, the linear correlation coefficient has been computed between the parallel- and cross-polarized returns, received simultaneously, to determine if a linear relationship exists between these two signals. [7] The coefficients which were computed were found to lie between -0.4 and +0.5, usually less than 0.2, for all types of trees observed and regardless of polarization at X-band.

E. Polarization Properties

A number of careful studies of the polarization properties of land clutter return have been conducted at X-band; however, no definitive experiments have been performed at frequencies above X-band. A number of operationally related clutter measurements have been made at K_u- and K_a-bands; however, these data are still classified due to the context in which they were obtained and are

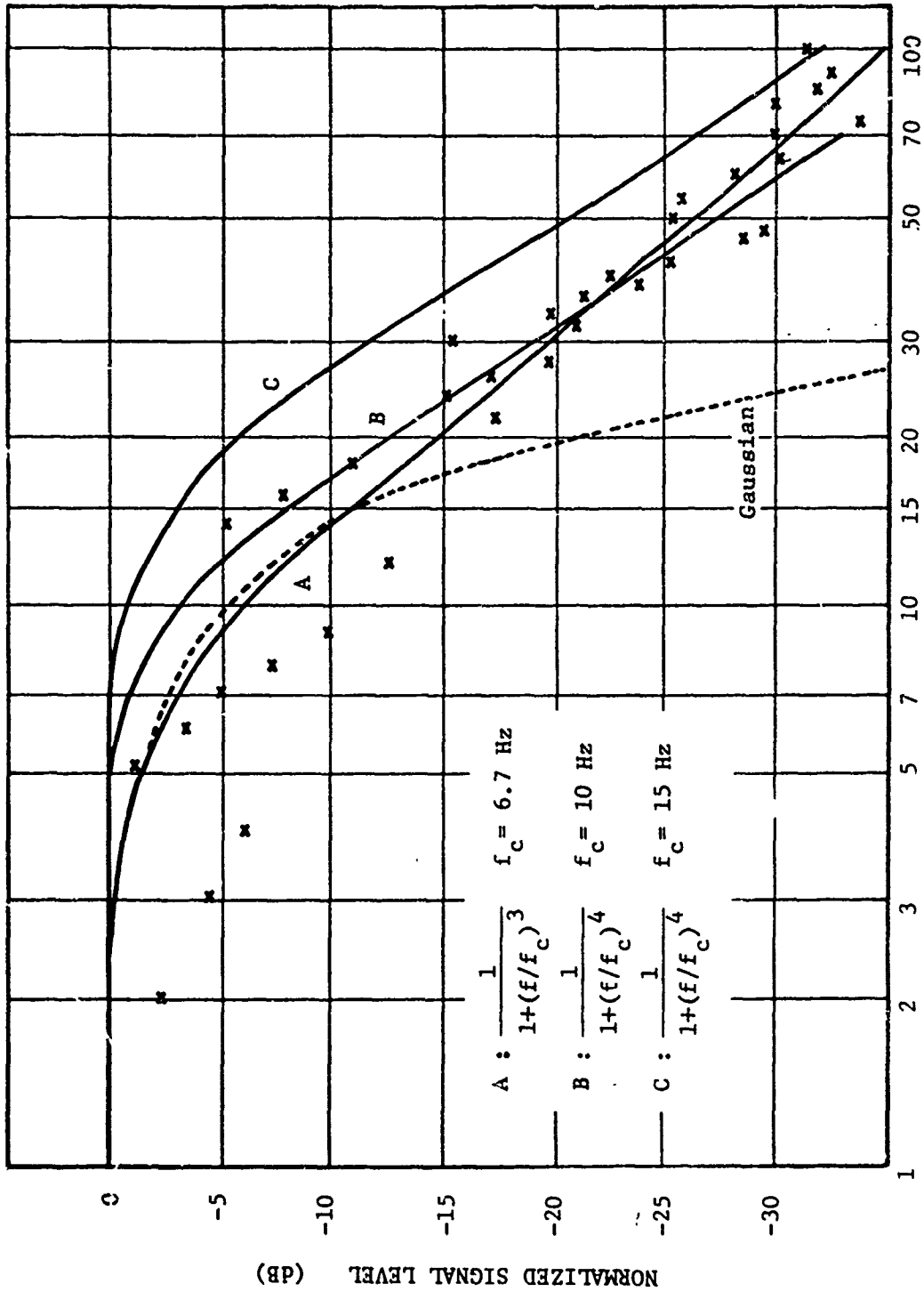

Figure 12. Clutter Spectra at X-Band. (After Fishbein Ref. 21)

not available for use in this report at the present time. Reference 7 includes one of the more comprehensive collections of polarization data currently available in the open literature. The primary emphasis of the clutter measurements included there is on tree return. One of the principal difficulties in interpreting the polarization data from tree returns is the variety of competing mechanisms which may contribute to the polarization properties of any given return. A detailed theoretical and experimental investigation was undertaken in the program reported on in Reference 7 in an attempt to determine the relative importance of such mechanisms. Some results of that investigation are reported below, including a discussion of a simple dipole model for describing the return from trees.

A collection of a large number, N, of dipoles randomly oriented and randomly distributed in space is used as a simple model for trees. Theoretical predictions of the polarization of radar return are made from this model. Note that range factors are suppressed throughout this discussion.

Consider a single dipole. A dipole reradiates that component of the incident field which can be resolved along the dipole axis. Hence, the magnitude of the received echo is proportional to the projection of the reradiated field of the dipole upon the direction of the received polarization.

Let θ be the angle between the horizontal and a vector along the dipole axis measured counterclockwise from the right. Then for a single dipole,

$$\begin{aligned} E^i_{HH} &= k \cos^2 \theta, \\ E^i_{HV} &= E^i_{VH} = k \cos \theta \sin \theta, \\ E^i_{VV} &= k \sin^2 \theta, \end{aligned} \tag{11}$$

where the first subscript on E, the received electric field, denotes the transmitted polarization, and the second subscript denotes the observed component of the return signal; k is a constant of proportionality. The powers of the return signals are

$$\begin{aligned} P^i_{HH} &= A \cos^4 \theta, \\ P^i_{HV} &= P^i_{VH} = A \cos^2 \theta \sin^2 \theta, \\ P^i_{VV} &= A \sin^4 \theta, \end{aligned} \tag{12}$$

For an ensemble of N dipoles, randomly oriented and incoherently phased, the scattered power from individual dipoles add. Thus,

$$P_{HH} = \sum_i P^i_{HH} = AN \langle \cos^4\theta \rangle = \frac{NA}{2\pi} \int_0^{2\pi} \cos^4\theta \, d\theta = \frac{3}{8} NA,$$

$$P_{HV} = P_{VH} = \sum_i P^i_{HV} = AN \langle \cos^2\theta \sin^2\theta \rangle = \frac{NA}{2\pi} \int_0^{2\pi} \cos^2\theta \sin^2\theta \, d\theta = \frac{1}{8} NA, \quad (13)$$

$$P_{VV} = \sum_i P^i_{VV} = AN \langle \sin^4\theta \rangle = \frac{NA}{2\pi} \int_0^{2\pi} \sin^4\theta \, d\theta = \frac{3}{8} NA.$$

Equations similar to these have previously been published by Hunter. [29] With the introduction of arbitrary relative phases, β and γ, the field components below are obtained from preceding equations where it is assumed that the return is just as likely to have equal powers in VV as HH. Adjustments to this concept will be made later.

$$E_{HV} = E_{VH} = \sqrt{AN/8}\, e^{j\beta},$$

$$E_{VV} = \sqrt{3\ AN/8}\, e^{j\gamma}. \quad (14)$$

These expressions lead to the following matrix equation:

$$\begin{bmatrix} E^r_H \\ \\ E^r_V \end{bmatrix} = \sqrt{AN/8} \begin{bmatrix} \sqrt{3} & e^{j\beta} \\ \\ e^{j\beta} & \sqrt{3}\, e^{j\gamma} \end{bmatrix} \begin{bmatrix} E^t_H \\ \\ E^t_V \end{bmatrix} \quad (15)$$

The superscripts r and t denote received and transmitted signals, respectively; the subscripts H and V denote the horizontal and vertical components of the wave, as before.

To represent circular transmission, let $E^t_V = E^t_H\, e^{\pm j\frac{\pi}{2}}$. Using this it can be shown that

$$E_D = \sqrt{AN/8} \left[\sqrt{3}\, E^t_H + 2E^t_H\, e^{j(\beta \pm \frac{\pi}{2})} - \sqrt{3}\, E^t_H\, e^{j\gamma} \right], \quad (16)$$

and

$$E_C = \sqrt{AN/8} \left[\sqrt{3}\, E^t_H + \sqrt{3}\, E^t_H\, e^{j\gamma} \right],$$

where the subscripts D and C denote the direct or parallel and the cross return, respectively. The corresponding powers are

$$P_D = \frac{1}{4} AN\,(E_H^t)^2 \left(5 - 3\cos\gamma + 2\sqrt{3}\left[\cos\left(\beta \pm \tfrac{\pi}{2}\right) - \cos\left(\beta - \gamma \pm \tfrac{\pi}{2}\right)\right]\right) \qquad (17)$$

and $$P_C = \frac{3}{4} AN(E_H^t)^2 \left[1 + \cos\gamma\right] .$$

The relative phase data which have been measured at X-band indicate that it is reasonable to assume that β, and $\beta - \gamma$, may be anywhere in the range from 0 to 2π with equal probability. The average power returns obtained from the preceding equations then become

$$\begin{aligned} \langle P_D \rangle &= \frac{1}{4} AN(E_H^t)^2 \left[5 - 3 \langle \cos\gamma \rangle\right] , \\ \text{and} \quad \langle P_C \rangle &= \frac{3}{4} AN\,(E_H^t)^2 \left[1 + \langle \cos\gamma \rangle\right] . \end{aligned} \qquad (18)$$

If the same distribution assumption is made about γ, the last two equations reduce to

$$\begin{aligned} \langle P_D \rangle &= \frac{5}{4} AN(E_H^t)^2, \\ \text{and} \quad \langle P_C \rangle &= \frac{3}{4} AN(E_H^t)^2. \end{aligned} \qquad (19)$$

If, on the other hand, γ is fixed and equal to zero, as might be intuitively expected, they reduce to

$$\begin{aligned} \langle P_D \rangle &= \frac{1}{2} AN(E_H^t)^2, \\ \text{and} \quad \langle P_C \rangle &= \frac{3}{2} AN(E_H^t)^2. \end{aligned} \qquad (20)$$

Equations 13 predict a polarization ratio of 4.8 dB for linear transmissions. Observed values lie between 4 and 8 dB; the larger values are plausible if effects of tree trunks are included.

For circular transmissions, Equations 19 and 20 are used to predict polarization ratios. These equations give a ratio of +2.2 dB when γ is randomly distributed and a ratio of -4.8 dB when γ equals zero. The parallel-to-cross ratios obtained from field measurements, which ranged from -1 to -4 dB, are not in agreement with either calculated value. It should be noted that the value of γ does not affect the polarization ratio or linearly polarized transmissions.

For all the X-band data reviewed under this study, investigators who looked at return powers P_{HH} and P_{VV} appear to state consistently that the horizontally polarized signals are 2 to 4 dB higher than the vertically polarized signals. The mean value obtained from Figure 13 shows σ^o_{HH} to be 2.5 dB higher than σ^o_{VV} for trees.

These data then would lead one to modify the matrix equation to read:

$$\begin{bmatrix} E_H^r \\ \\ E_v^r \end{bmatrix} = \sqrt{AN/8} \begin{bmatrix} \sqrt{3} & e^{j\beta} \\ \\ e^{j\beta} & \sqrt{\frac{3}{2}}\, e^{j\gamma} \end{bmatrix} \begin{bmatrix} E_H^t \\ \\ E_v^t \end{bmatrix} \tag{21}$$

and for circular transmission and reception

$$\begin{aligned} E_D &= \sqrt{AN/8}\left[\sqrt{3} + 2e^{j\beta\pm\pi/2} - \sqrt{\frac{3}{2}}\, e^{j\gamma}\right] E_H^t \\ E_C &= \sqrt{AN/8}\left[\sqrt{3} + \sqrt{\frac{3}{2}}\, e^{j\gamma}\right] E_H^t \end{aligned} \tag{22}$$

The resulting equations for power are

$$\begin{aligned} P_D &= 1/8\ AN\ (E_H^t)^2 \left[\frac{17}{2} + 4\sqrt{3}\cos(\beta\pm\pi/2) - \frac{6}{\sqrt{2}}\cos\gamma - 4\sqrt{\frac{3}{2}}\cos(\beta-\gamma\pm\pi/2)\right] \\ P_C &= 1/8\ AN\ (E_H^t)^2 \left[\frac{9}{2} + \frac{3}{2}\cos\gamma\right]. \end{aligned} \tag{23}$$

From collected data, it appears reasonable to assume β is random and takes on any value between 0 and 2π with equal probability, and that γ is close to zero. Thus the ratio of average powers, $\langle P_D\rangle/\langle P_C\rangle$, will be -1.9 dB for this condition. This is in agreement with field measurements as presented in Figure 14.

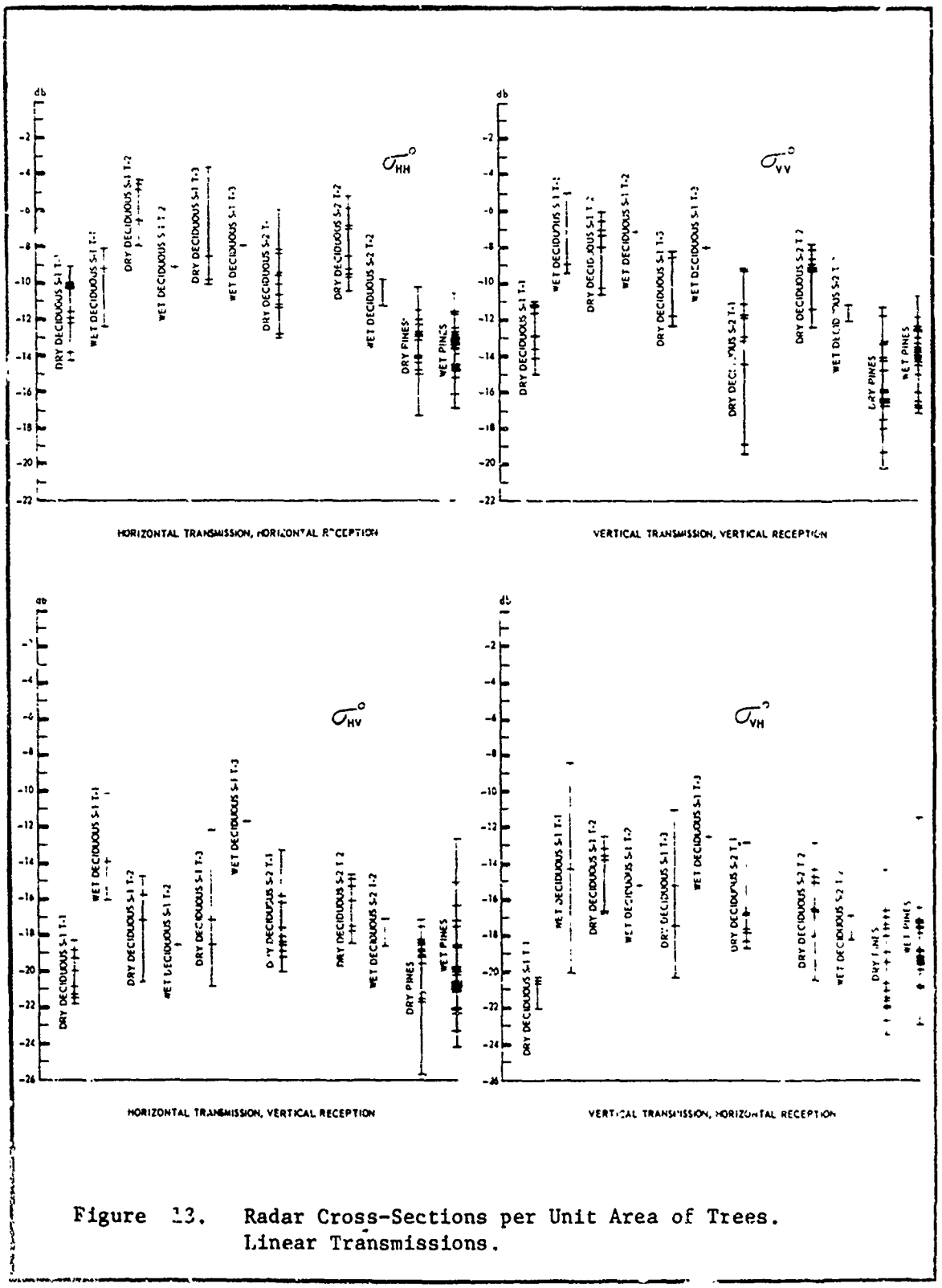

Figure 13. Radar Cross-Sections per Unit Area of Trees. Linear Transmissions.

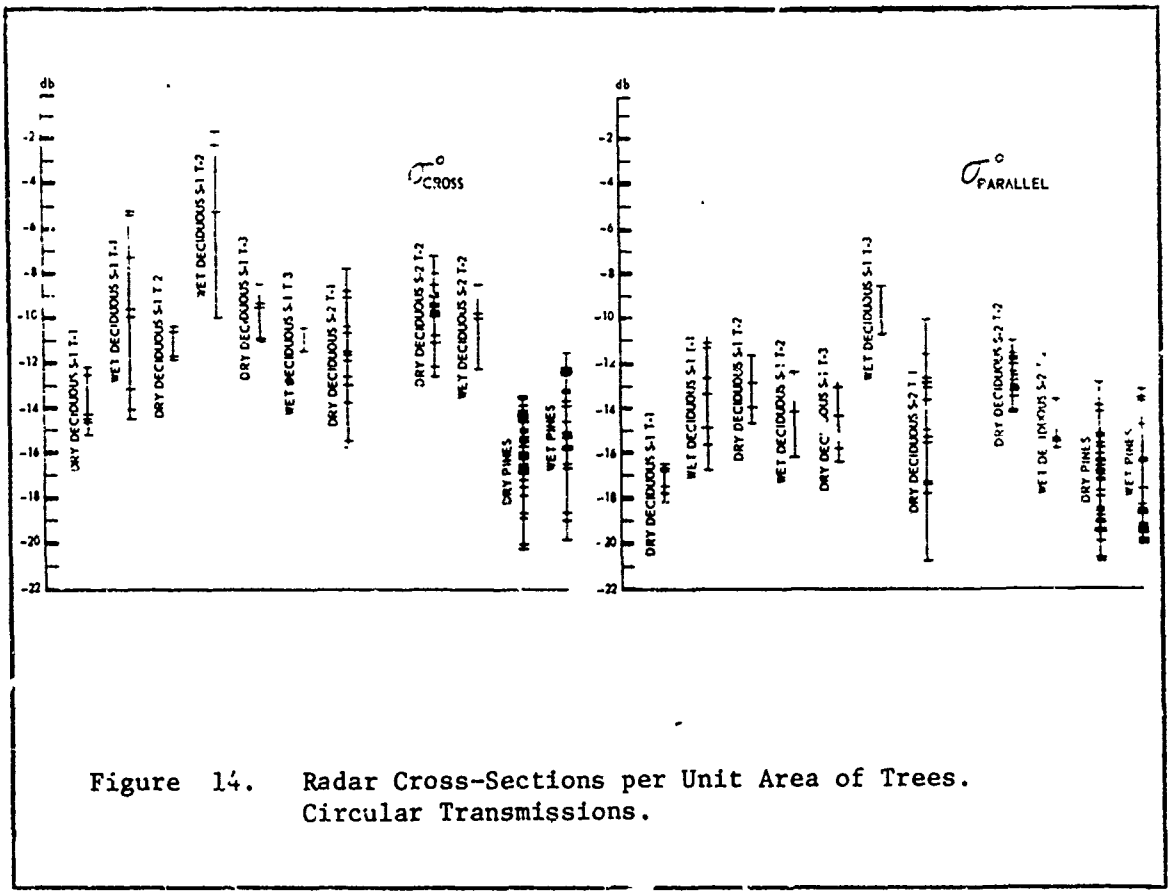

Figure 14. Radar Cross-Sections per Unit Area of Trees. Circular Transmissions.

III. CLUTTER EFFECTS ON SYSTEM PARAMETER CHOICE

The ultimate weight and size of a radar will depend very strongly on the frequency of operation, as both component size and power consumption vary inversely with frequency (for a given upper bound of performance). The choice of operating frequency depends on a number of factors, including allowable antenna aperture, maximum range, weather performance, anticipated target-to-clutter ratios, and the anticipated processing gains which may be obtained with that choice. The key factor in system sizing considered in this report is the behavior of the clutter return as a function of frequency; the objective of this section is to place the results of the clutter-return investigations described above in perspective with the general requirements of an airborne fire-control radar system.

Limited comparative data are available on the cross-section of various man-made targets although a number of independent investigations have been made of target returns at the various frequencies of interest in this study. The general tendency is for the effective cross-sections of vehicles, buildings, and personnel to be approximately independent of frequency above 9 GHz. The assumption used in the considerations below is that cross-section is not frequency dependent.

The initial question to be answered is the effect of frequency scaling on maximum detection range. It is necessary to establish an acceptable set of ground rules for such a comparison; however, the detailed treatment of such a comparison is beyond the scope of this study. General considerations for guiding the comparison of frequency effects on system parameters can be found in several radar handbooks. [30, 31] Given a knowledge of available transmitter power, receiver noise figure, and losses as a function of frequency it is possible to make order-of-magnitude performance comparisons which will bound the anticipated system capability. For the airborne fire-control radar, it is anticipated that antenna size (and therefore gain) will be a critical factor. If a constant aperture size of 20 inches is assumed (limited by air-frame considerations), the resulting azimuth beamwidths and gains are given in Table V.

The antenna gains resulting from the assumption above, along with limiting values of transmitter power and receiver noise figure can be used in the

TABLE V.

Antenna Characteristics at Three Frequencies for 20-inch Aperture

	Circular Aperture		Rectangular Aperture	
Wavelength	Beamwidth (3dB)	Gain	Beamwidth (3dB)	Gain
3.2 cm	4.14^{o}	27.4 dB	3.21^{o}	28.5 dB
8.6 mm	1.11^{o}	33.1 dB	0.862^{o}	34.2 dB
3.2 mm	0.414^{o}	37.4 dB	0.321^{o}	38.5 dB

usual radar equation

$$R = \left[\frac{P_t G^2 \lambda^2 \sigma}{(4\pi)^3 \, kT_o B \, \overline{NF}_o L \, (S/N)} \right]^{1/4}, \qquad (24)$$

to give a bound to the maximum detection ranges for each frequency as illustrated in Figures 15, 16, and 17. Table VI is a summary of the radar parameters assumed in preparation of Figures 15 through 17. The band of anticipated performance indicates the spread resulting from system compromises and field degradation which can reasonably be expected. These performance curves are for clear weather and represent an upper bound of performance, since such factors as operator effectiveness and clutter masking have not been included. A significant aspect of the predictions shown in Figures 15, 16, and 17 is that maximum detection ranges are approximately independent of frequency with the constant aperture constraint. These figures also include indications of general range of cross-section of several classes of target.

There are two key aspects of impact of clutter on the detection of a target by radar: (1) masking and (2) false alarms. A consideration of the cross-section per unit area summaries given in Section II above, together with the resolution cell which results from the 20inch aperture constraint and a pulse length of 50 nsec (25-foot resolution), results in the anticipated clutter cross-sections summarized in Table VII.

The predictions of average effective cross-section for several classes of clutter summarized in Table VII are based on the mathematical representations of σ^o tabulated in Section II rather than on specific experimental data. Comparisons of the predicted values of cross-sections for clutter in Table VII with the target cross-sections indicated in Figures 15 through 17 suggests that, on the basis of average cross-section alone, clutter should not be a major limitation to the detection of targets by any of the example radars. However, it must be pointed out that the extrapolations in frequency and grazing angle used to obtain the data in Table VII are very sensitive to the actual behavior of clutter return. The required experimental data are not available at this time to substantiate the mathematical predictions.

The problem of detection in clutter is further complicated by the statistical nature of the return. Discussions of the return from trees in Section II indicate that under some circumstances amplitude distributions

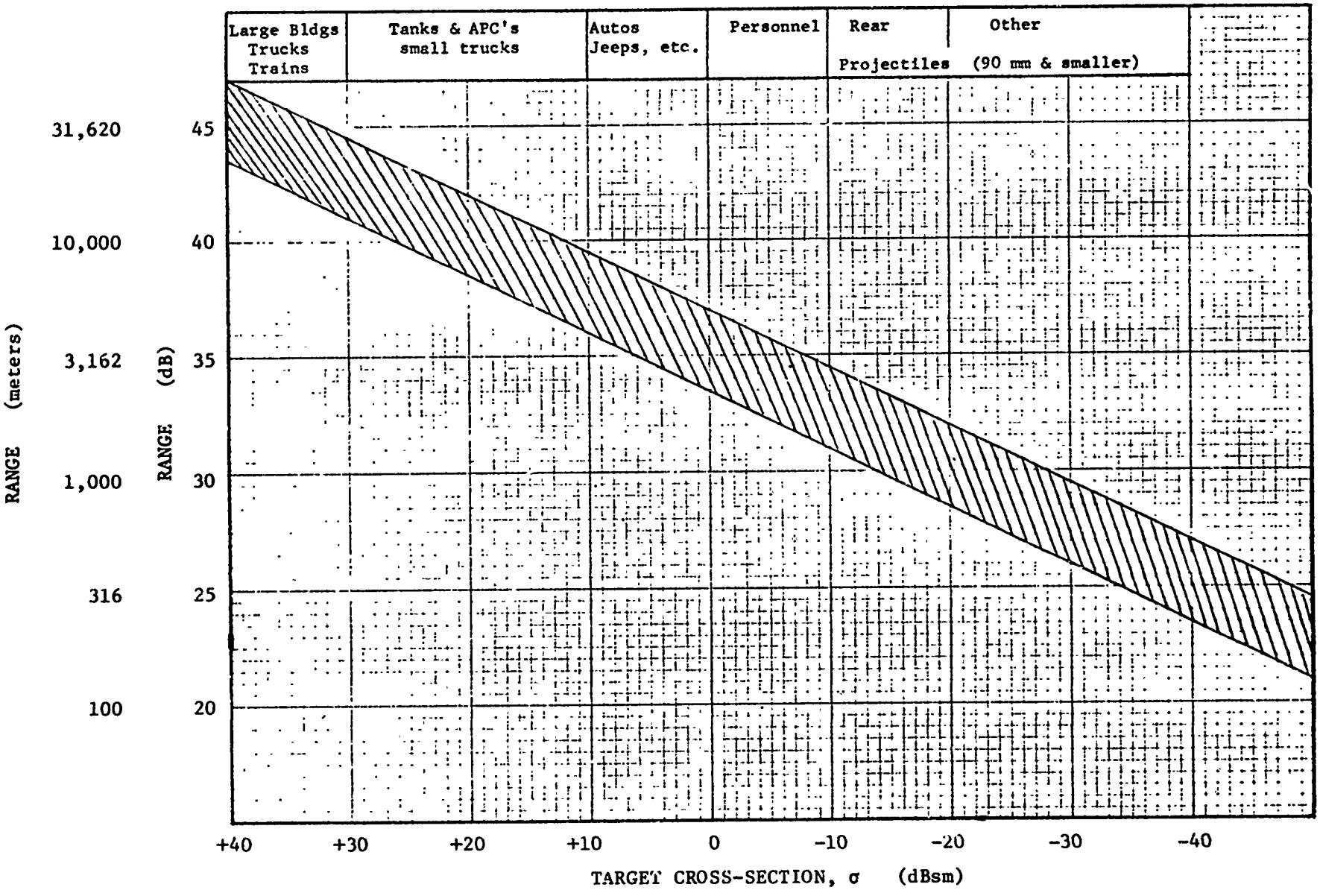

Figure 15. Projected Performance of an Airborne Fire Control Radar Operating at X-Band (32 mm).

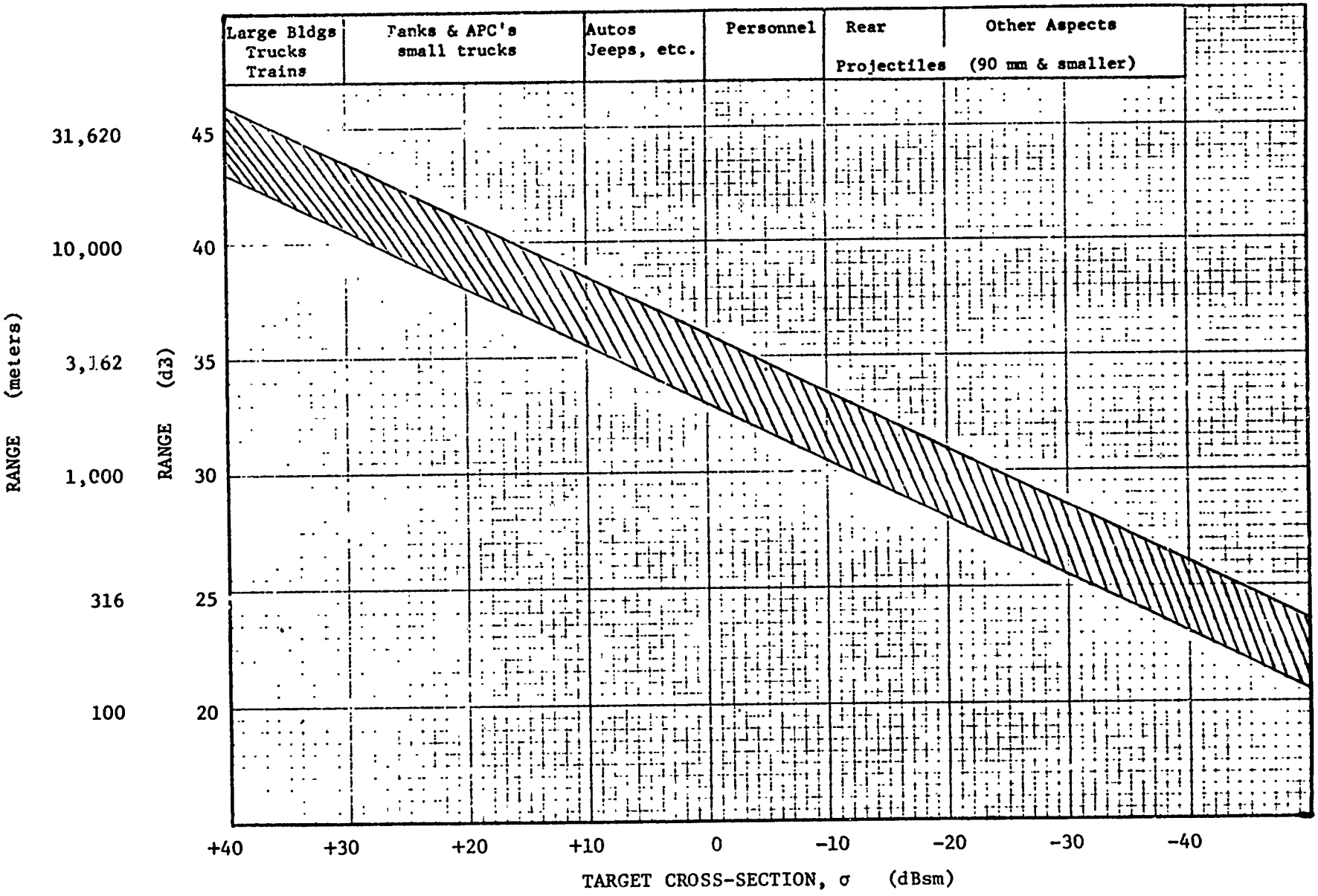

Figure 16. Projected Performance of an Airborne Fire Control Radar Operating at K_a-Band (8.6 mm).

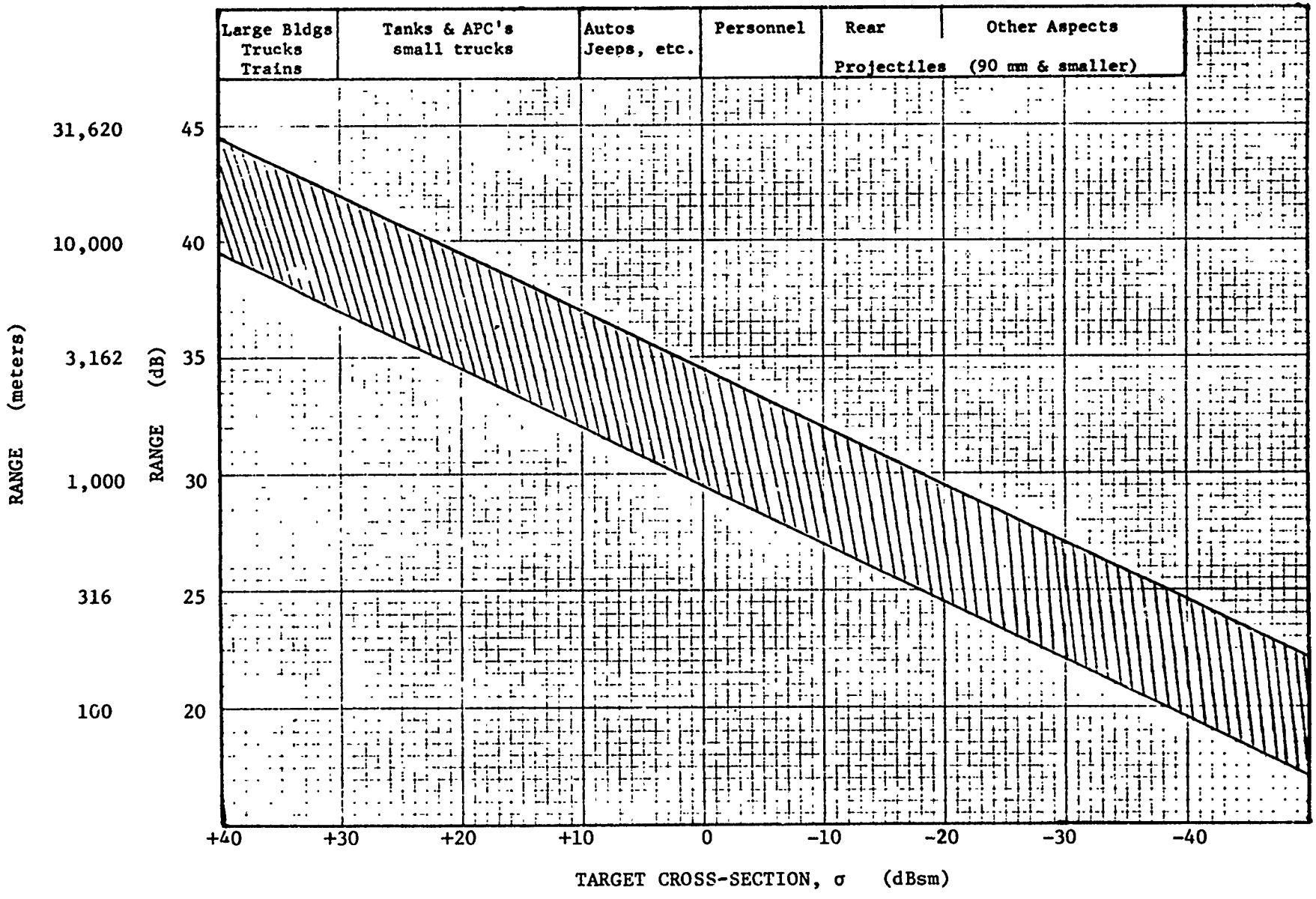

Figure 17. Projected Performance of an Airborne Fire Control Radar Operating at V-Band (3 mm).

TABLE VI.

Example Sets of Radar Parameters

Parameter	Value Assumed		
Wavelength, λ	32 mm	8.6 mm	3 mm
Transmitted Power, P_t	100 KW	60 KW	4 KW
Antenna Gain, G	27 dB	33 dB	37 dB
Pulse Length, τ	50 nsec	50 nsec	50 nsec
Bandwidth, B	20 MHz	20 MHz	20 MHz
Noise Figure, $\overline{NF}_o$	8 dB	8 dB	10 dB
Loss (T/R), L	2 dB	4 dB	6 dB
Signal-to-Noise (single hit), S/N	13 dB	13 dB	13 dB

TABLE VII.
Estimated Clutter Cross-Sections for Two Grazing Angles

Grazing Angle*	Wavelength	Clutter Area	Effective Cross-Section			
			Forest	Grass	Open Land	Snow
10°	3.2 cm	24 dBsm	-5 dBsm	-13 dBsm	-16 dBsm	-17.5 dBsm
10°	8.6 mm	18 dBsm	-6.9 dBsm	-14 dBsm	-16 dBsm	-16 dBsm
10°	3.2 mm	14 dBsm	-6.5 dBsm	-13 dBsm	-15 dBsm	-16 dBsm
1°	3.2 cm	33 dBsm	-12 dBsm	-20 dBsm	-18 dBsm	-24 dBsm
1°	8.6 mm	26 dBsm	-15 dBsm	-22 dBsm	-17 dBsm	-24 dBsm
1°	3.2 mm	23 dBsm	-14 dBsm	-20 dBsm	-12 dBsm	-21 dBsm

*Aircraft is assumed to be at 1000 feet.

might be obtained which behave as a log-normal distribution with large standard deviation. Three example sets of Receiver Operating Characteristic curves are shown in Figures 18, 19, and 20. These figures illustrate the impact on the detection problem which results when the extension is made from a non-fluctuating target in receiver (Rayleigh) noise to the case of a log-normally distributed clutter background and either a non-fluctuating target or a log-normally distributed target.

For example, consider the difference in performance implied in the cases shown in Figures 18 and 19. For a false alarm rate of 10^{-6}, the required signal-to-background ratio increases by more than 15 dB when the background clutter is similar to that illustrated in Figure 7. Figure 20 illustrates the greatly reduced possibility of achieving very high probabilities of detection when returns from both target and background are log-normally distributed. If a probability of detection of 80% is required with a false-alarm probability of 10^{-6}, a clutter background of trees, and a moderately fluctuating target (i.e., Figure 20), then a target cross-section of 20 dBsm or more will be required for the example radars illustrated in Figure 15, 16, and 17.

These illustrations can be extended to other cases; however, the real detection problem is further complicated by the fact that ground return can include a significant number of specular returns of rather large amplitude and which can appear very much like targets at all frequencies and grazing angles for which observations have been reported. These false targets will act to increase the effective false alarm rate beyond that indicated by statistical considerations alone, thus detailed system performance investigations will require careful consideration of the non-statistical returns, particularly at millimeter wavelengths as the effective cross-section of such scatters will be quite sensitive to the apparent reflectivity, which may change considerably with frequency.

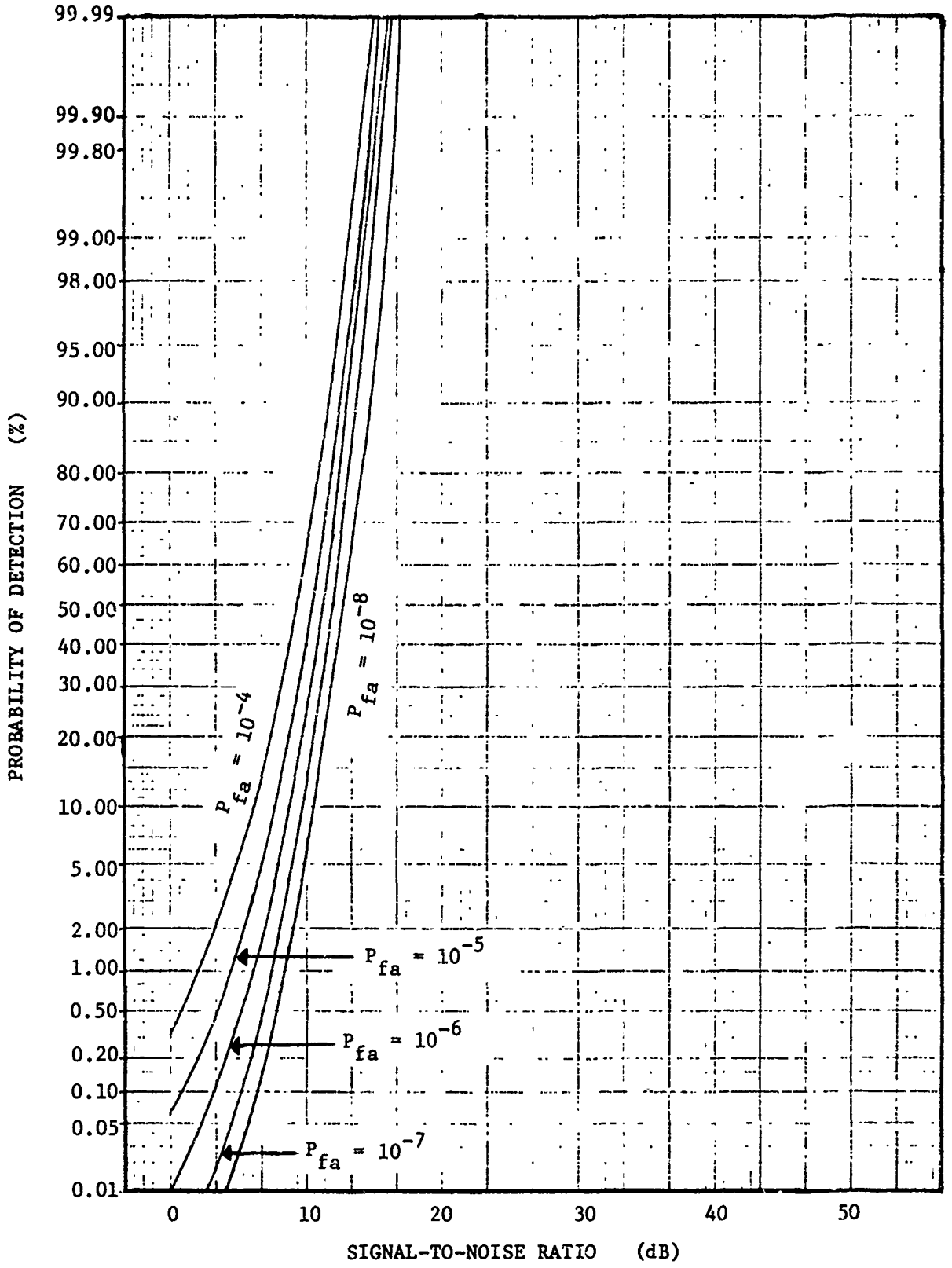

Figure 18. Receiver Operating Characteristic for Nonfluctuating Target in a Noise (Rayleigh) Background. Detection Based on a Single Received Pulse.

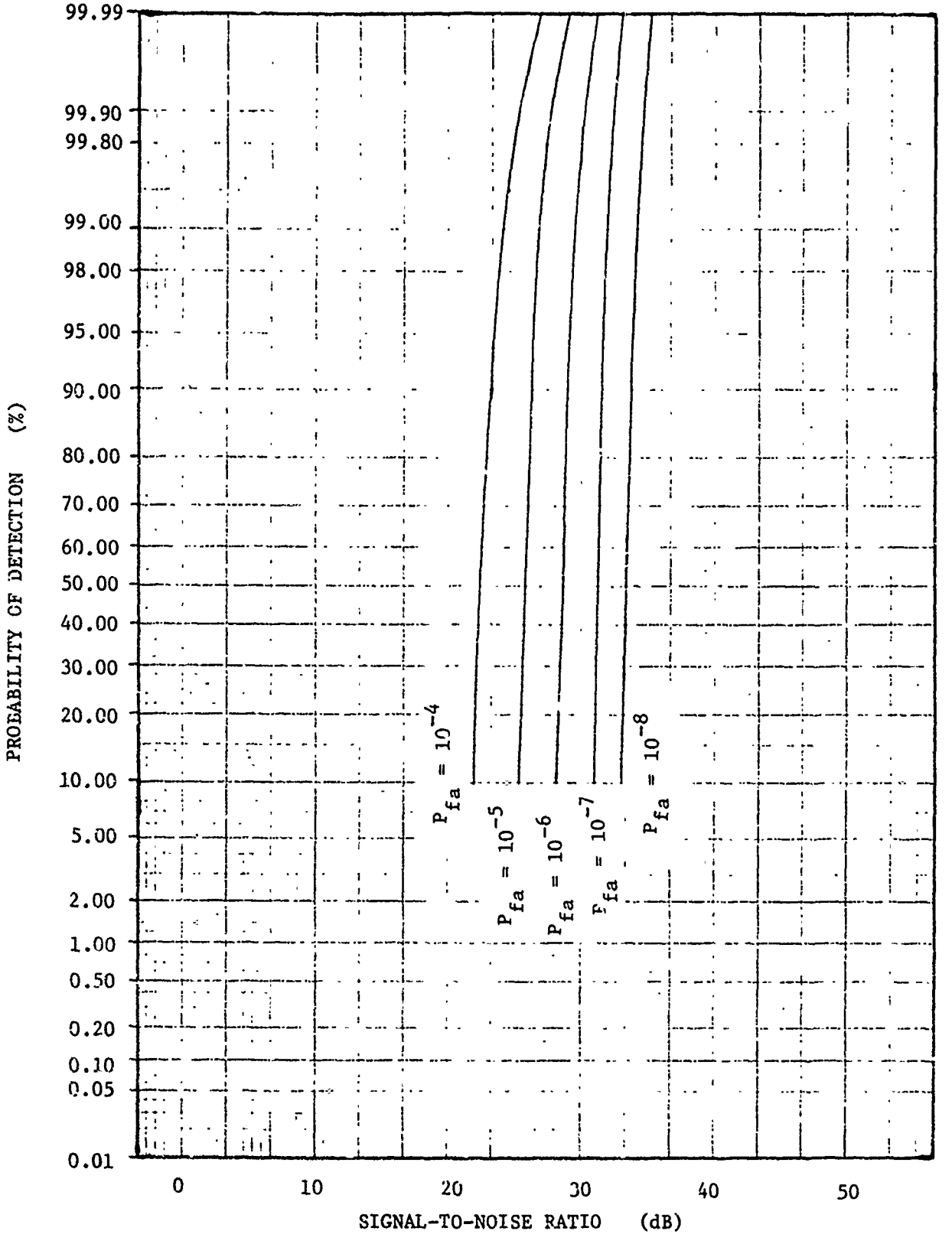

Figure 19. Receiver Operating Characteristic for Nonfluctuating Target and a Log-Normally Distributed Clutter. Standard Deviation of 6 dB Was Used for the Clutter. Detection Based on a Single Received Pulse.

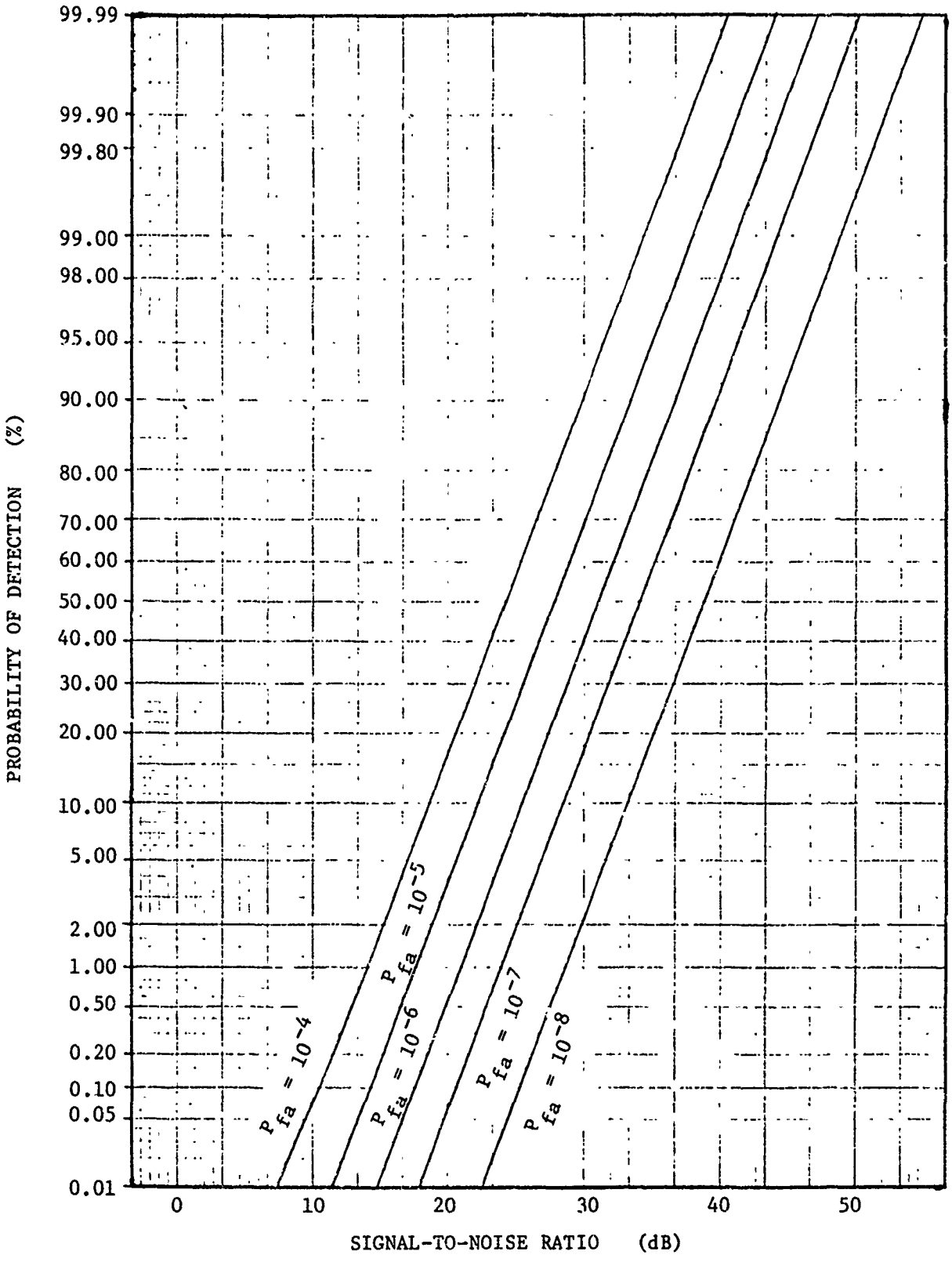

Figure 20. Receiver Operating Characteristic for Log-Normal Target and Clutter. Standard Deviations of 4.34 dB for the Target and 6.5 dB for Clutter were used. Detection Based on a Single Received Pulse.

IV. SUMMARY AND RECOMMENDATIONS

The data assembled in this report have been selected from a review of the currently available unclassified literature. Care was taken to subject each data set individually to tests of internal consistency and physical "reasonableness." Experimental methods and data formats were checked and the data finally used in the summaries were weighted according to the estimated relative quality of the source as determined from this critical review. Finally, the overall summaries were reviewed for consistency and, in cases of question, the original source documents were rechecked.

The resulting summaries of radar cross-section have been used as guidelines for the specification of preliminary forms of mathematical representations for cross-section per unit area (σ^o) for a variety of clutter types and for the amplitude statistics of the return from foliage. Current representations are suitable for use in exploring basic system trade-offs.

The salient aspects of the findings assembled in this report can summarized as follows.

1. Very few quantitative data are available in the literature which describe the behavior of ground-clutter return for frequencies above those of X-band.

2. Few data on the radar cross-section of clutter have been reported for grazing angles below 10^o.

3. Limited data are available at X-band to describe the spectral and polarization behavior of clutter returns; however, no data on these characteristics are available at higher frequencies.

4. The cross-section per unit area of clutter types which are "rough" (i.e., trees, large crops, etc.) is consistently larger for all grazing angles and frequencies than that of "smooth" clutter (i.e., plowed ground, snow, water, etc.).

5. The cross-section per unit area of all classes of clutter tends to be reduced as the grazing angle approaches zero; however, the apparent roughness, and therefore the rate at which it decreases, is a function of frequency.

6. The statistics of the parallel polarized returns for which data exist indicates that, in general, a Rayleigh distribution is <u>not</u> a suitable descriptor because measured distributions contain more large amplitude returns than would be predicted by the Rayleigh function.

7. A log-normal distribution can be suitably fitted to the measured distributions; however, the truncation or limiting of maximum amplitude which actually occurs physically must be determined separately from measurements.

8. For cases where observations have been made of the orthogonally polarized components of the return, the statistics of the quadrature received polarization are approximately described by the Rayleigh function.

9. The data available at X-band on the spectral behavior of the magnitude of clutter returns suggest that a power law function is a better fit to the higher frequency tail than is the commonly used Gaussian function.

10. Examination of representative sets of receiver operating characteristics suggest that, for false alarm rates in the range of 10^{-4} to 10^{-8}, as much as 20 dB more return from a target will be required for a given probability of detection with a background of log-normal tree returns as compared to Rayleigh noise.

As a result of the investigations on this program, the following recommendations are offered.

1. The clutter cross-section data and mathematical representations assembled herein should be used to provide preliminary algorithms for development of computer models of clutter return for use in establishing baseline system parameters.

2. No calibrated data exist at grazing angles between zero and 15^{c} at frequencies above X-band. Therefore a data collection program should be undertaken to fill this gap.

3. The effects of atmospheric conditions, especially of precipitation, need to be determined and incorporated in the clutter and system performance programs.

4. The new data obtained under (2) and (3) should be used to extend the current mathematical models for clutter.

5. Specific experiments should be designed and appropriate field operations should be conducted for the purpose of defining the usefulness of polarization and spectral techniques for enhancement of target detection and recognization.

V. REFERENCES

1. "Polarization characteristics of Radar Targets," C. H. Currie, R. D. Hayes and M. W. Long, Final Report on DA 36-039 SC-56761, Georgia Institute of Technology, March 1955, AD 55 124.

2. "Backscattering from Water and Land," C. R. Grant and B. S. Yaplee, Proceedings of the IRE, Vol. 45 July 1957, pp. 976-982.

3. "NRL Terrain Clutter Study, Phase II," S. C. Daley, W. T. Davis, J. R. Duncan and M. B. Lasing, NRL Report 6749, Naval Research Laboratory, Washington, D.C. 21 October 1968.

4. "Terrain Backscatter Measurements at 40 to 90 GHz," H. E. King, C. J. Zamites, Jr., D. E. Snow, R. I. Collition, IEEE Transactions on Antennas and Fropagations, AP-18, No. 6, November 1970, pp. 780-784.

5. "Radar Cross-Section Measurements of Snow and Ice for Design of SEV Pilotage System," P. Hoekstra and D. Spanogle, Cold Regions Research and Engineering Laboratory, Hanover, New Hampshire, June 1971.

6. "Radar Mapping in Heavy Rain with Orthogonal Radar Modes at X- and K_a -Band," M. S. Wheeler and K. A. Badetscher, NAECON 70 RECORD, 1970, pp. 72-80.

7. "Study of Polarization Characteristics of Radar Targets," R. D. Hayes and J. R. Walsh, Jr., Final Report on DA 36-039 SC-64713, Georgia Institute of Technology, October 1958, AD 304 957.

8. "Analysis of Target Recognition for Airborne Groundpaint Radars," G. I. Sillman, Report RLT-3830-8 on AF 33(616)-5114, Volume 2 (Eight Triannual Report), Motorola, April 1960, AD 316 798.

9. "k_u - Band Terrain Measurements of Grazing Incidence (U)," A. Nichols and H. Amble, Report 2144-80-T (Project MICHIGAN) on DA 36-039 SC-52654, University of Michigan, Institute of Science and Technology, June 1957, AD 138 911.

10. "Terrain Contract (U)," Report 694-8 (Summary Engineering Report) on AF 33(616)-3649, Ohio State University Research Foundation, Antenna Laboratory, 31 December 1957, AD 1652 787.

11. "Terrain Return Measurements and Applications (U)," R. C. Taylor, R. L. Cosgriff, and W. H. Peake, Report 694-11, on AF 33(616)-3649, Ohio State University Research Foundation, Antenna Laboratory 30 April 1959.

12. "Terrain Contract (U)," Report 694-13 (Final Engineering Report) on AF 33(616) 3649, Ohio State University Research Foundation, Antenna Laboratory, 15 June 1959, AD 309 610.

13. "Radar Terrain Return (Task 2.1--Advanced Fuzing-REST Program) (U)," G. A. Baker, Report RAD-TM-62-103 on AF 04(694)-239, Avco Corporation Research and Advanced Development Division, 19 January 1963, AD 335 679.

14. "A Summary of Measurements and Theories of Radar Ground Return (U)," R. H. Bond, Report TM-655 on NOw-60-0366-C, Hughes Aircraft Co,. September 1960, AD 349 643L.

15. "Elevation-Angle Dependence of Radar Ground Return (U)," Charles H. Wilcox, Scientific Report 5, on AF 19 (604) - 1708, Hughes Aircraft Company, 31 March 1957, AD 117 042.

16. "Review of Theories and Measurements of Radar Ground Return (Supplement) (U)," E. A. Wolff, Report CRC-5198-3 on AF 19 (604) - 5198, Electromagnetic Research Corporation, 29 February 1960, AD 316 627.

17. "Terrain Clutter Measurements (U)," F. C. MacDonald, W. S. Ament, and D. L. Ringwalt, NRL Report 5057, Naval Research Laboratory, 21 January 1958, AD 156 184.

18. "Terrain Return Measurements at K_a - Band (U)," R. C. Taylor Report 694-6 on AF 33(616)-3649, Ohio State University Research Foundation, Antenna Laboratory, 15 November 1957, AD 149 737.

19. "Radar Terrain Return Study, Final Report: Measurements of Terrain Back-Scattering Coefficients with an Airborne X-band Radar," Report GERA-463 on NOas-59-6186-C, Goodyear Aerospace Corporation, 30 September 1959, AD 229 104.

20. "Ground Echo," R. K. Moore, Radar Handbook, M. I. Skolnik, Editor, McGraw-Hill Book Co., New York, 1970, Chapter 25.

21. "Clutter Attenuation Analysis," W. Fishbein, et al., Tech Report TM-2808, U. S. Army Electronics Command, March 1967, AD 665 352.

22. "Low-Angle Radar Sea Return at 3-mm Wavelength," W. Rivers, Final Report on Contract N62269-70-C-0489, Georgia Institute of Technology, 15 November 1970.

23. Threshold Signals, J. L. Lawson and G. E. Uhlenbeck, MIT Radiation Laboratory Series, Volume 24, McGraw-Hill, New York, 1950, p. 53.

24. "Methods of Solving Noise Problems", Bennett, Proceedings of the IRE, 44, No. 5, 1936, p. 609-638.

25. Advanced Calculus for Engineers, Hildebrand, Prentice-Hall, Inc., New York, 1949, p. 353.

26. Radar Design Principles, F. Nathanson, McGraw-Hill, New York, 1969, pp. 148-154.

27. "Detection Probabilities for Log-Normally Distributed Signals," G. R. Heidbreder and R. L. Mitchell, IEEE Trans. on Aerospace and Electronic Systems, AES-3, No. 1, January 1967, pp. 5-13.

28. The Log-Normal Distribution, J. Aitchison and J. A. C. Brown, Cambridge University Press, London, Eng., 1966.

29. "The Polarization Characteristics of Certain Radar Echoes at X-Band," I. M. Hunter, T.R.E. Technical Note No. 196, Telecommunications Research Establishment, August 1953, p. 15.

30. Radar System Analysis, D. K. Barton, Prentice-Hall, Inc., Englewood Cliffs, N.J., 1964.

31. Radar Handbook, M. I. Skolnik, Editor, McGraw-Hill Book Co., New York, 1970.

VI. RELATED BIBLIOGRAPHY

1. "Radar Reflectivity (U)", D. E. Roberts, Report CRD 2137 on 6/PROJ/7338/Cb 32(a), Decca Radar, Ltd. (Great Britain), September 1960, U. K. Confidential-Discreet, U. S. Confidential, Excluded from GDS, AD 323 6221.

2 "Radar Reflectivity (Volume 2) (U)", A. A. Geale, Report SRL 2973 on KO/P/0302/CB 21, Decca Radar, Ltd. (Great Britain) (a), 17 October 1963 U.K. Secret-Discreet, U.S. Secret, Excluded from GDS, AD 345 295.

3. "Target Signature Study Interim Report. Volume 1: Survey (U)," R. R. Legault and T. Limperis, Report 5698-22-T(I) on AF 33(657)-10974, University of Michigan, Institute of Science and Technology, October 1964, Confidential, Excluded from GDS, AD 354 166.

4. Quarterly Report (WASDD-TN-59-231 (VII), "DACOR. Advanced Data Correlator Study and Development (U)," Report GER-10165 on AF 33(616)-6409, Goodyear Aerospace Corporation, 20 January 1961, Secret, Excluded from GDS, AD 325 687.

5. "Overland AEW Radar Study (U)," Hughes Aircraft Co., NOw-60-9366-C, 1960-1961, Confidential (formerly Group 4).

6. "An Approach to Radar Target Classification Through-Polarization-Simulation Techniques (U)," R. D. Tompkins, NRL Report 5579, Naval Research Laboratory, 23 January 1961, Confidential, Excluded from GDS, AD 321 802.

7. "Reflection and Doppler Characteristics of Targets and Clutter (U)," E. G. Meyer, S. N. Broady, G. H. Smith, et al., Semi-Annual Report 1 on DA 28-043 AMC-00263 (E), Radiation Inc., 31 December 1964, Confidential, Excluded from GDS.

8. "Reflection and Doppler Characteristics of Targets and Clutter (U)," J. E. Butler, Final Report on DA 28-043 AMC-00263(E), July 1967, Confidential, Excluded from GDS, AD 383 221.

9. "High Altitude Terrain Contour Data Study (U)," J. C. Marshall, J. L. Martin, T. F. Ryan, and D. M. Skidmore, Report EB-5261-0305 on AF 33(616)-8143, Sperry Gyroscope Company, August 1963, Confidential (formerly Group 4), AD 343 980.

10. "Target Signature Study (U)," R. F. Goodrich, B. A. Harrison, and G. Rabson, Quarterly Reports 5172-2-Q, 5172-3-Q, and 5172-4-Q on DA 36-039 SC-90733, University of Michigan Radiation Laboratory, Confidential, Excluded from GDS, (2) AD 335 122, (3) AD 339 165, (4) AD 348 875.

11. "Low Altitude Capability Study (U)," Final Engineering Report on AF 33(616)-5228, DYD-40167, Westinghouse Electric Corporation, May 1958, Confidential (formerly Group 4), AD 315 397.

12. "Polarization and other Properties of Radar Echoes (U)", I. M. Hunter, Technical Note 628, Royal Radar Establishment-Great Britain, September 1957, Secret, Excluded from GDS, AD 161 662.

13. "Bi-Static Ground Scatter Measurements in X-band and the Ground Scatter Jammer Parameters (U)", B. J. Starkey, Report S957-104-3 (DEW), Royal Canadian Air Force, 26 September 1963, Secret, Excluded from GDS, AD 355 237.

14. "Coherent High-Resolution Radar Interpretation and Analysis Techniques Study (U)", Final Report [GERA] (RADC-TDR-64-185) on AF 30(602)-3079, Goodyear Aerospace Corp., August 1964, Secret, Excluded from GDS, AD 355 237.

15. "Aural Presentation of AI Radar Terrain Reflections for Velocity Measurement by Means of Doppler Shift (NV)," Technical Memorandum 207/58, Canadian Armament Research and Development Establishment, September 1958, Secret, Excluded from GDS, AD 303 541.

16. "Notes on the Radar Visibility of a Tank (U)", K. A. Lauire, Technical Memorandum 306/60, March 1960, Secret, Excluded from GDS, AD 318 179.

17. "Ambush Detection (U)," Report TR-5, Army Limited War Laboratory, August 1964, Secret, Excluded from GDS, AD 354 364.

18. "Fluctuations of Ground Clutter Return in Airborne Radar Systems (U)", H. H. Shara, Report BRL 2138 on 6/PROJ/7338/CB 32(a), Decca Radar, Ltd. (Great Britain) November 1960, U. K. Restrickted, U.S. Confidential MHA-1, AD 323 623L.

19. "Short Pulse Techniques for Personnel Detection in Vegetation Clutter (U)", R. R. Apgar, M. A. Schmidt, H. H. Laue, and R. E. Beitz, Report R-64-021 on DA 04-495 AMC-522(R), General Dynamics Electronics, 1964, Confidential, (formerly Group 4), AD 356 566.

20. "Final Report. Generic Ranging Study. Volume 2 (U)", E. L. Berger, Report ASER 37-61 on DA 36-034-507 ORD-2925, General Electric Company, Defense Systems Department, 15 February 1962, Confidential, (formerly Group 4), AD 328 760.

21. "Field Trials Report (U)" Report SRK2022, 6/WT/4996 . 4 (b)3, Decca Radar, Ltd. (Great Britain), 1 March 1960, AD ,686.

22. "Notes on the Radar Visibility of a Tank (U)", K. A. Laurie, Technical Memorandum, Canadian Armament Research & Development Establishment, March 1960, Secret, Excluded from GDS, AD 318 179.

23. "Measurement of the Backscattering Cross-Section of an M4A2 Sherman Tank at X and K Bands (U)," R. S. Larsen, Technical Memorandum, Canadian Armament Research and Development Establishment, April 1960, Secret, Excluded from GDS, AD 319 295.

24. "Microwave Reflection from Targets and Terrain: A Survey of the Literature (U)", K. A. Lauire, Technical Memorandum, Part I (Text) and Part II (Appendix), Canadian Armament Research and Development Establishment, May 1960, Secret, Excluded from GDS, AD 321 924 and AD 321 925.

Unclassified
Security Classification

DOCUMENT CONTROL DATA - R & D

Security classification of title, body of abstract and indexing annotation must be entered when the overall report is classified)

1 ORIGINATING ACTIVITY (Corporate author)	2a. REPORT SECURITY CLASSIFICATION
Engineering Experiment Station Georgia Institute of Technology Atlanta, Georgia 30332	Unclassified
	2b. GROUP

3 REPORT TITLE

Land Clutter Characteristics for Computer Modeling of Fire Control Radar Systems

4 DESCRIPTIVE NOTES *(Type of report and inclusive dates)*

Technical Report Number 1

5 AUTHOR(S) *(First name, middle initial, last name)*

Robert D. Hayes and Frederick B. Dyer

6 REPORT DATE	7a. TOTAL NO OF PAGES	7b. NO OF REFS
15 May 1973	54	55

8a. CONTRACT OR GRANT NO	9a. ORIGINATOR'S REPORT NUMBER(S)
DAAA 25-73-C-0256	
b. PROJECT NO	
c.	9b. OTHER REPORT NO(S) *(Any other numbers that may be assigned this report)*
d.	

10 DISTRIBUTION STATEMENT

None

11 SUPPLEMENTARY NOTES	12 SPONSORING MILITARY ACTIVITY
Georgia Tech Project A-1485	Frankford Arsenal Philadelphia, Pennsylvania 19137

13 ABSTRACT

Summarized in this report are the pertinent, unclassified data on the reflectivity of a variety of classes of land clutter. The data are confined to those taken at radar frequencies included between 9 and 95 GHz. Brief discussions are included for a number of the characteristics of radar return from clutter, although emphasis is directed to the average statistics of the amplitude of the return. Prelminary mathematical representations are included which describe: (1) average radar cross-section per unit area (σ^o), (2) amplitude statistics of the return, (3) spectral behavior of received power , and (4) polarization properties of the return from foliage. Also included is a discussion of some of the effects of the characteristics of land clutter on the choice of system parameters and on the nature of the problem of target detection in clutter.

DD FORM 1 NOV 65 1473 (PAGE 1)

S/N 0101-807-6801

Unclassified
Security Classification

14 KEY WORDS	LINK A		LINK B		LINK C	
	ROLE	WT	ROLE	WT	ROLE	WT
Radar						
Cross-Section						
Land Clutter						
Statistics						
Polarization						
Modeling						
Algorithm						
Millimeter						